

BACHELOR THESIS

Injection locking of lithium diodes

EBERHARD-KARLS UNIVERSITY OF TÜBINGEN
Department of Physics

July 8, 2021

Contents

1	Introduction	1
2	Theory of laser injection locking	2
2.1	Semiconductor laser diodes	2
2.1.1	p-n junction	2
2.1.2	Fabry-Perot laser diode and interferometer	3
2.1.3	External cavity diode laser	5
2.2	Driven oscillator model for injection locking	5
2.3	Mode-matching with the Gaussian beam model	6
2.3.1	Properties of a Gaussian beam	6
2.3.2	Gaussian beam propagation using ABCD-matrices	8
3	Experimental setup	9
3.1	Setup with optical parts	9
3.2	Instrument control	10
4	Characterization of a 660 nm Thorlabs diode	11
4.1	Free-running laser diode	11
4.1.1	Wavelength tuning	11
4.1.2	Lasing threshold	12
4.2	Beam shaping	12
4.3	Demonstration of injection locking	15
4.3.1	Current dependency	15
4.3.2	Lasing threshold in injection locked state	18
5	Characterization of a 675 nm Ushio laser diode	20
5.1	Free running diode	20
5.1.1	Wavelength tuning	20
5.1.2	Lasing threshold	20
5.2	Beam shape and coupling efficiency	21
5.3	Demonstration of injection locking	23
5.3.1	Current dependency	23
5.3.2	Current-temperature stability maps	25
5.3.3	Lasing threshold in injection locked state and variation of seed power	28
5.3.4	Minimizing seed power	29
6	Active stabilization of injection locking	32
7	Conclusion	33
8	Acknowledgements	35

1 INTRODUCTION

1 Introduction

In cold atom experiments for laser cooling and trapping of atoms, laser powers of more than 100 mW are often required. This ensures enough scattering events in a Zeeman slower by maximizing the power broadening of the absorption lines. Furthermore, magneto-optical traps, while loading, are in need of sufficient power to reduce the number of atoms lost on the way [MS07]. The output power of an external cavity diode laser does not produce enough output power for such applications. Alternatively, tapered amplifiers are a way to produce sufficient output power. These are currently not available for the targeted laser cooling wavelength for lithium of 671nm. However, injection locking of free-running, high power diodes is an alternative to tapered amplifiers for delivering enough output power. [SED19]

This is a technique to produce higher output power at a stable frequency. To achieve this, a weak signal of typically a few mW of an external cavity diode "seed" laser is injected into a free-running "slave" diode, which is capable of higher output power. Although the diode has a broad emission spectrum at most currents and temperatures applied to it, single-mode output with a narrow line width and a stable frequency can be reached by injecting light from the seed. Stable injection locking strongly depends on the mode-matching between the seed and the slave laser diode beam, sufficient incoupled seed power to the laser diode cavity, and the difference between the seed laser frequency and the resonance of the slave diode cavity. [SED19]

The goal of this work is to find a stable injection lock setup with over 100 mW of output power. There are two diodes characterized for this aim while injection locking them. One is available at Thorlabs (L660P120) with a center wavelength of 660 nm and up to 120 mW of output power in the free-running state. The other diode manufactured by Ushio (HL67xx1DG) is not yet readily available on the market but has a center wavelength of 675 nm with up to 0.25 W of output power and can be directly operated at 671 nm by lowering the temperature. There are concerns that this temperature would be below the dew point, especially in summer. This causes condensation on the diode from the water vapor in the air, explaining why this diode is tested only via the second approach.

This report is structured as follows: In Section 2 a short introduction into semiconductor laser physics is explaining the working principle of laser diodes. Additionally, the injection locking theory and the Gaussian beam model are discussed. The experimental setup and instrument control are described in Section 3. This is followed by the characterization of the Thorlabs diode with a center wavelength of 660 nm in Section 4 and the Ushio diode with a center wavelength of 675 nm at appropriate temperatures in Section 5. An outlook on further improving the setup by actively stabilizing the injection lock is given in Section 6.

2 THEORY OF LASER INJECTION LOCKING

2 Theory of laser injection locking

Injection locking was reported on as early as the 17th century when Christiaan Huygens, confined to bed by illness, noticed that the pendulums of two clocks on the wall moved in the same way if the clocks were hung close enough to each other. He was able to explain the locking between the two clocks by attributing it to the coupling to mechanical vibrations transmitted through the wall. [Sie86]

The phenomenon of injection locking can occur in any oscillatory system, including electrical oscillators, whether mechanical or biological machines as well as lasers. [Raz03]

In the case of lasers, whereas a weak beam of the seed laser is injected into a free-running slave diode, the frequency of the slave can follow the seed frequency phase-locked. This happens only if the frequency discrepancy between the slave diode and the seed laser is low enough and the modes of both beams are matched [SED19].

Often when a laser is run far away from its free-running state by using an external cavity, the frequency and output can change easily. This is why an external cavity diode laser is often stabilized at a small output power and then injected into a free-running laser diode, which is temperature and current stabilized. A small fraction of the output power is sufficient to reach stable injection locking. The basic building blocks for both the external cavity diode laser and the free-running slave diode are semiconductor laser diodes. [Zim19]

2.1 Semiconductor laser diodes

Semiconductor lasers have become the most frequently used type of laser in the past few decades. This development was followed by the mass distribution of CD and DVD and optical fiber communications. [Zim19] Cost efficient compact devices are available with typical dimensions of a few millimeters. The emission wavelength can range from blue to the far infrared [Sil96].

For semiconductor lasers, quantum transitions are characterized by the band properties of the semiconducting material. These materials are mainly elements from Groups III -VI of the periodic table such as GaAs, the predominant material for near-infrared light sources. Usually semiconductor materials, which are used for laser operations, have direct band gaps where the radiative transition probability is higher compared to indirect band gaps. This is due to the fact that the momentum is conserved for direct band gaps but not for indirect band gaps. The momentum of a photon simply is infinitesimal and is not sufficient to have an electron converting to a hole with different momentum [Sze81]. These diode lasers are operated by passing an electrical current through the gain medium in a forward direction. The current can then be easily modulated, which results in an efficient modulation of the lasing output. [WH91]

2.1.1 p-n junction

A laser diode is typically comprised of a p-n junction diode, where electrons from the n-doped material drift to the p-doped material filling the excess holes here. Hereby, the n-doped side is getting positively charged and the p-doped side negatively. Meanwhile, the energy bands in the p-doped region are shifted up by the electrostatic energy necessary to get the electrons from the n- to the p-region. The energy band stops shifting when the equilibrium is reached i.e. the valence band of the p-doped region is on the same energy level as the one of the conducting band of the n-doped region. Close to the contact region, the number of electrons is increasing in the conducting band as the number of holes in the valence band is decreasing. [WH91]

Current through the active layer in a forward direction i.e. positive voltage at the p-doped side leads to a decrease of the jump in potential from p to n. Electrons and holes thus are able to

2 THEORY OF LASER INJECTION LOCKING

get closer to the active layer in which electrons and holes recombine resulting in light emission. The energy of the emitted light is given by the energy band gap of the material in use. [Zim19]

This figure has been removed by GRIN for copyright reasons.

Figure 1: Construction of a semiconductor laser diode. Taken from [WH91]

2.1.2 Fabry-Perot laser diode and interferometer

In addition to a p-n junction, Fabry-Perot laser diodes are equipped with a Fabry-Perot cavity. This laser cavity comprises of two parallel ends of the semiconductor which act like mirrors along the crystal axis. The semiconductor builds the gain medium inbetween. The low-reflectivity front facet, which is partially transmitting, and the highly reflecting back facet of the semiconductor are usually optically coated to minimize losses. The emission spectrum of an optical laser diode is relatively broad and can exhibit several longitudinal modes. Therefore, lasing at different frequency modes is supported by Fabry-Perot laser diodes resulting in different wavelengths of the emitted light. [WH91]

Fabry-Perot laser diodes are typically manufactured so that the optical beam is confined in a waveguide with a single spatial mode. However, as described above, several frequency modes occur for laser diodes. The spacing of the frequency modes is given by

$$\Delta\nu_{\text{FSR,LD}} = \frac{c}{n \cdot 2L} \quad (1)$$

where c is the speed of light, L is the length of the laser diode chip and n is the refractive index of the semiconductor waveguide. [SED19]

The frequency modes and their output power are determined by the material used for the gain medium, the forward current being applied to it, and the temperature. Tuning temperature affects the energy band gap of the semiconductor material in use. Thus, the output power and wavelength of the emissioned light from the diode can be altered. Stimulated emission can be greatly influenced by the current applied to the gain medium of the laser diode. Increasing current results in more stimulated emission. Above a threshold value, spontaneous emission is playing a greater role and starts competing with stimulated emission. This is unfavorable for the reason that spontaneous emission again is unpolarized. Therefore, staying close to the operational current and within the operating range of current, stimulated emission is upheld as the dominant transition type. [Sze81]

The homojunction laser diodes described above were later advanced to heterojunction laser diodes, which relaxed the need for cryogenic temperatures [Mes08].

2 THEORY OF LASER INJECTION LOCKING

In general, a Fabry-Perot interferometer is a cavity with the simplest configuration consisting of two parallel reflecting mirrors with one of them being partially transmitting. A signal can be obtained behind the cavity only if it is resonant with the cavity. A standing wave is produced within the cavity. Constructive interference then occurs if the light inside the cavity is in phase with the light which enters the cavity. The cavity length can be tuned with a modulation voltage applied to a piezo crystal attached to one of the cavity mirrors. The free spectral range $\Delta\nu_{FSR}$ of light circulating inside the Fabry-Perot cavity is given by

$$\Delta\nu_{FSR} = \frac{c}{2L} \quad (2)$$

where c is the speed of light, L the length of the cavity and the refractive index is approximated with $n \approx 1$. [Sil96]

The ratio of transmitted light I_t to incident light I_i for a Fabry-Perot cavity is described by

$$\frac{I_t}{I_i} = \frac{1}{1 + (\frac{2}{\pi})^2 F \sin^2 \left(\frac{\Delta\phi}{2} \right)} \quad (3)$$

where $\Delta\phi$ is the phase factor of the wave travelling in the cavity and F defines the finesse [Mes08]. The finesse is a measure of quality of the resonator and is given by the ratio of the free spectral range $\Delta\nu_{FSR}$ and the line width $\Delta\nu_{FWHM}$

$$F = \frac{\Delta\nu_{FSR}}{\Delta\nu_{FWHM}} = \frac{\pi\sqrt{R}}{1-R} \quad (4)$$

where R is the reflectivity of the mirror [Sil96].

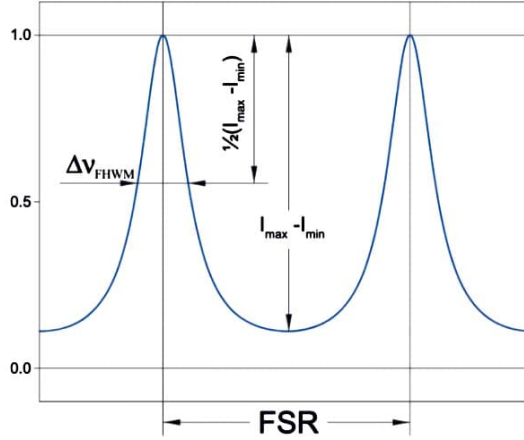


Figure 2: Transmission signal of a Fabry-Perot cavity. Taken from [Did16]

Similarly, the quality factor Q of a Fabry-Perot cavity is a measure of peak sharpness given by

$$Q = \frac{\nu_0}{\nu_{FWHM}} \quad (5)$$

where ν_0 is the center frequency of a peak in the mode spectrum [Sil96].

2 THEORY OF LASER INJECTION LOCKING

2.1.3 External cavity diode laser

Within the injection lock setup, an external cavity diode laser in catseye configuration is in use as the master laser. The frequency-selective element in the catseye configuration is an etalon, an optical filter, in comparison to the Littrow-configuration, in which a grating is used [WH91]. A piezo can move a partially transmitting mirror along the optical axis so that the wavelength of the laser is tuned. Longitudinal modes are suppressed by the etalon filter between the mirror and the laser. Only light in a narrow frequency range can pass this filter. A lens at a distance of one focal length is positioned in front of the mirror resulting in the catseye configuration together with the mirror. Behind the mirror, another lens is positioned for collimation of the divergent beam. [Zim19]

2.2 Driven oscillator model for injection locking

In injection locking, the injected laser beam from the master laser locks the phase and frequency of the slave laser diode. It can be thought of as similar to an external cavity diode laser in which the output is constrained to a certain frequency. The model of a driven oscillator can be applied to the slave laser diode.

The following discussion is based on [Sie86] and was initially done for a ring laser to separate the input and output beam easily. Additionally, this can be expanded to a different laser setup in which light is injected into a laser diode.

The parameters for the oscillator, in this case the slave laser diode itself, are: the unconstrained frequency of the slave laser diode ω_0 and the intensity of the output beam I_0 . The driving frequency of the injected signal associated with the seed laser is ω_1 and the intensity I_1 . The phase-amplitude equations for the time-varying amplitude of the cavity signal and the time-varying phase inside the cavity are given by

$$\frac{dE(t)}{dt} + \frac{\gamma_c - \gamma_m}{2} E(t) = \gamma_e E_1(t) \cos[\phi(t) - \phi_1(t)] \quad (6)$$

$$\frac{d\phi(t)}{dt} + \omega_1 - \omega_0 = -\gamma_e \frac{E_1(t)}{E(t)} \sin[\phi(t) - \phi_1(t)] \quad (7)$$

where $E(t)$ is the amplitude of the electric field inside the cavity and $E_1(t)$ of the injected signal, γ_c the cavity decay, γ_e the external cavity decay rate due to external coupling to an output mirror and γ_m the growth rate. The phase of the field inside the cavity is described by $\phi(t)$ and of the seed signal by $\phi_1(t)$.

A steady-state output condition so that all derivatives satisfy $\frac{dE(t)}{dt} = \frac{d\phi}{dt} = 0$ is defined as the injection locked state of the driven oscillator. The amplitude of the cavity signal then oscillates with the natural frequency ω_0 . The phase lock can be described with Eq. 7 and a few approximations applied to it which are not further specified here (see [Sie86]). The injection lock behavior is then expressed by

$$\frac{d\phi(t)}{dt} + \omega_1 - \omega_0 = -\omega_m \sin[\phi(t)] = -\frac{\omega_0}{Q_e} \sin[\phi(t)] \sqrt{\frac{I_1}{I_0}}. \quad (8)$$

This steady-state output condition can only be satisfied by the following constraint on the frequency difference between the seed laser and the slave laser diode

$$-\omega_m \leq (\omega_1 - \omega_0) \leq \omega_m.$$

Thus, ω_m is the maximal excursion the frequency of the injected signal ω_1 from the driven oscillator resonance frequency ω_0 can make before the steady-state output is lost. The injection

2 THEORY OF LASER INJECTION LOCKING

locking bandwidth, i.e. the frequency range over which the seed frequency can be tuned above and below the resonance frequency ω_0 while maintaining the injection lock, is given by

$$\Delta\omega_{\text{lock}} \equiv 2\omega_m = \frac{2\omega_0}{Q_e} \sqrt{\frac{I_1}{I_0}} \quad (9)$$

where Q_e is the Q-factor of the external cavity of the ring laser model. The injection locking range for laser diodes usually lies within a few nm, extending both above and below the seed frequency [Zim19].

Solutions to the "Adler-equation" in Eq. 8 are also available outside of the injection locking bandwidth where the output from the driven oscillator contains both the injected and the following free-running signal. If the injected signal frequency ω_1 gets closer to the resonance frequency ω_0 , it can occur that the frequency of the following signal is pulled inside the steady-state injection locking range. Other interesting phenomena also start appearing when the injected signal frequency is just outside of the locking range, like a growing number of distortion sidebands developing in the Fourier spectrum of the following laser cavity signal.

Equivalently, the injection lock bandwidth for laser injection locking is described in [MOJ85] by

$$\Delta\omega_{\text{lock}} = \eta \cdot \nu_{\text{FSR,LD}} \cdot \sqrt{\frac{P_i}{P_0}} \sqrt{1 + \alpha^2} \quad (10)$$

where η is the injection locking efficiency taking values between 0 and 1, $\nu_{\text{FSR,LD}}$ is the free spectral range of the laser diode cavity given in Eq. 1, P_i and P_0 are the power of the injected seed light and the output power of the slave laser diode measured in front of the diode, α is the line width enhancement factor specific to the semiconductor gain medium.

2.3 Mode-matching with the Gaussian beam model

For the seed mode to be amplified in the slave diode, the modes need to be well matched to the internal cavity of the slave diode. Then all other spontaneous modes existing in the slave diode are suppressed across the whole gain medium and only the seed mode is amplified. Here, single-mode output with the same narrow line width of the seed laser can be achieved. Therefore, properties of the beam such as the divergence angle can be abstracted from both beams and manipulated with beam shaping optics. The following discussion of the properties and propagation of a Gaussian beam is based on [Sil96].

2.3.1 Properties of a Gaussian beam

With the Gaussian beam model, properties can be abstracted from the slave and seed laser beams. An ideal Gaussian-shaped beam can be completely characterized at any location by its beam waist and wavefront curvature at one specific location. If a beam has a Gaussian beam profile at one specific location, it will have the Gaussian beam profile at any location. This implies that laser resonators generate Gaussian beams because the beam within the cavity has a Gaussian spatial distribution at the mirrors of the resonator.

The beam waist is the minimal spatial extension a Gaussian beam has. The following parameters associated with the Gaussian beam spatial extension and the angular divergence are represented in Fig. 3. The propagation occurs along the z-axis here. For every unaltered Gaussian beam, this focus point is reached at some location in space. After passing a lens, the Gaussian beam minimum waist is reached at the focal length. The beam waist in a resonator occurs inbetween the two mirrors e.g. in a confocal resonator, the beam waist is reached halfway through the resonator. The Gaussian beam expands from the point of the beam waist and a divergence in

2 THEORY OF LASER INJECTION LOCKING

the linear regime can be defined. The beam waist at a distance of $\pm z$ from the minimal beam waist if the minimal focus point is set to $z = 0$ is described by

$$w(z) = w_0 \sqrt{1 + \left(\frac{z}{z_0}\right)^2} \quad (11)$$

where z_0 is the Rayleigh range, also referred to as the depth of focus, is in terms of wavelength λ and the minimal beam waist w_0 defined by

$$z_0 = \frac{\pi w_0^2}{\lambda} . \quad (12)$$

The beam wavefront at a given location z is of the form

$$R(z) = z \left[1 + \left(\frac{z_0}{z} \right)^2 \right] . \quad (13)$$

The divergence of a Gaussian beam can be described by the full angle at a given location z , where the beam has reduced to half of its maximum intensity at the center of the beam and is defined by

$$\theta(z) = \lim_{z \rightarrow \infty} \frac{2w(z)}{z} . \quad (14)$$

Of course, real laser beams can exhibit higher-order modes and be differently shaped from a Gaussian beam, but in a good approximation this model can be applied to the seed and slave diode lasers because single-spatial-mode operation is present in the injection lock setup. For the fundamental TEM₀₀-mode the beam is Gaussian-shaped. The Gaussian transverse distribution of a simple Gaussian beam is given by

$$I(\rho, z) = I_0 e^{-2\left(\frac{\rho}{w(z)}\right)^2} \quad (15)$$

where I_0 is the maximum intensity and ρ the transverse coordinate.

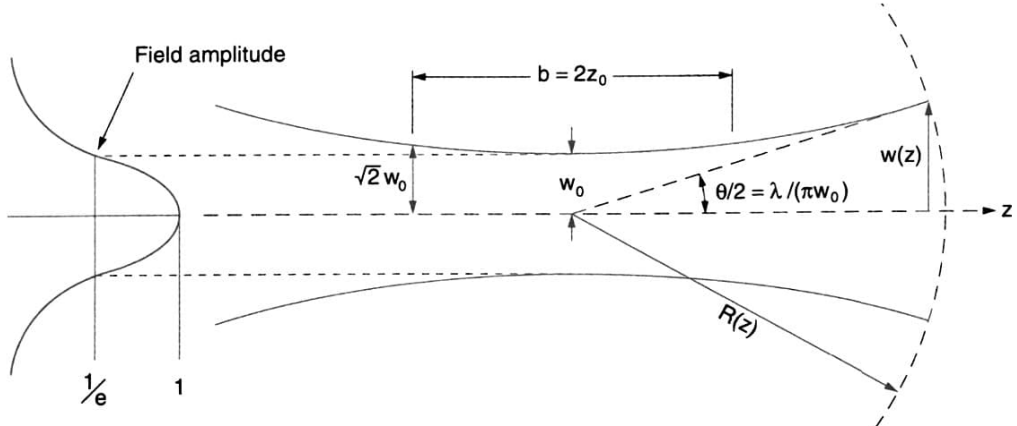


Figure 3: Gaussian beam parameters. Taken from [Sil96]

2 THEORY OF LASER INJECTION LOCKING

2.3.2 Gaussian beam propagation using ABCD-matrices

The properties of an unaltered Gaussian beam are described in 2.3.1. It is possible to calculate the manipulation of a Gaussian beam with the help of ABCD-matrices through mirrors, lenses and other optical elements. The calculation with an ABCD-matrix is based on the complex beam parameter q defined in terms of the Gaussian beam curvature $R(z)$, the wavelength λ and the beam waist at a specific location $w(z)$

$$\frac{1}{q} = \frac{1}{R(z)} - j \frac{\lambda}{\pi w^2(z)} . \quad (16)$$

Thus, ABCD-matrices can be used for calculation of the complex beam parameter at an arbitrary point q_2 if it is given at a different point with q_1 as follows

$$q_2 = \frac{Aq_1 + B}{Cq_1 + D} . \quad (17)$$

A ray of light is characterized by its $x(z)$ - and $y(z)$ component and by its divergence $\theta_x(z)$ and $\theta_y(z)$ along both axes if elliptically shaped. For describing the beam radius and divergence along the x-component perpendicular to the optical axis and y-component, respectively of an elliptically shaped beam after passing a spherical lens, the ABCD-matrix for this calculation is given by

$$\begin{pmatrix} x_2 \\ \theta_{x,2} \end{pmatrix} = \begin{pmatrix} 1 & 0 \\ -\frac{1}{f} & 1 \end{pmatrix} \begin{pmatrix} x_1 \\ \theta_{x,1} \end{pmatrix} \quad (18)$$

where x_2 and $\theta_{x,2}$ are the position and divergence after propagation and x_1 and $\theta_{x,1}$ before propagating through a spherical thin lens [Sie86]. This equation is analogous for the y-component of the beam. This simplifies for a round beam where there is no need to treat the x- and y - component of the beam separately.

3 EXPERIMENTAL SETUP

3 Experimental setup

The optical parts for the injection lock setup are assembled starting after the external cavity diode laser (ECDL) output from a single-mode fiber. Optical parts are arranged to produce a high output power through injection locking and to diagnose the beam output with the instruments described below.

3.1 Setup with optical parts

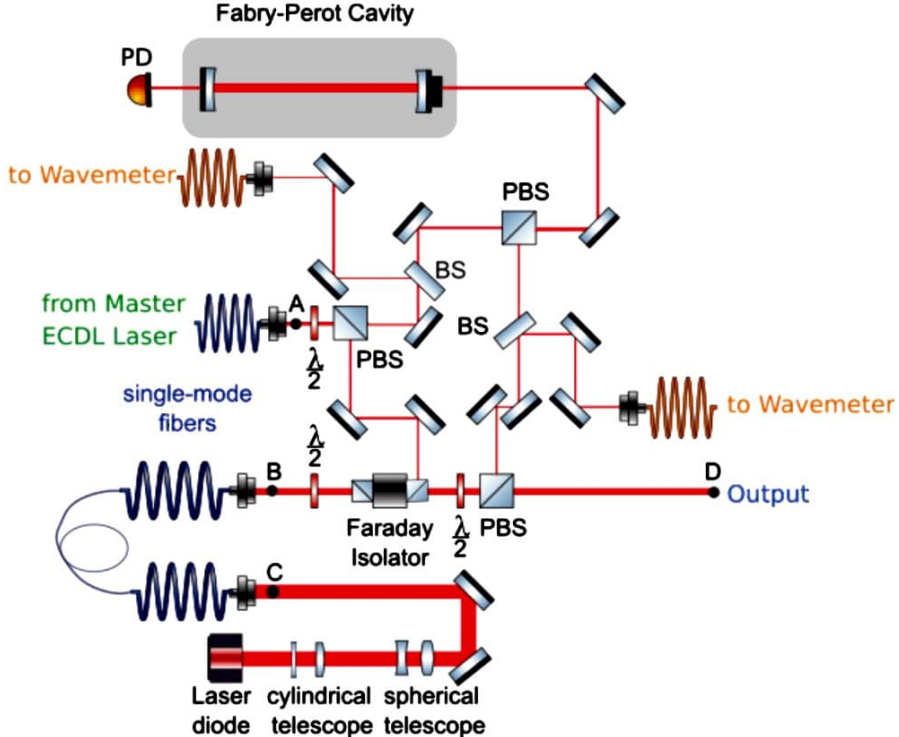


Figure 4: Experimental setup

Utilized as the seed laser is an ECDL in cat eye configuration. The wavelength is stabilized at roughly 671 nm and can be detuned by a piezo attached to the front mirror. For the injection lock setup, the ECDL is operated at 140 mA and 23 °C. The output then is just below 30 mW. Through a fiber from the ECDL breadboard to the injection lock breadboard, 13 mW measured at the point A in Fig. 4 are preserved. A half waveplate is introduced just after the fiber and in front of a PBS to split off the beam for monitoring the wavelength at the wavemeter and the mode spectrum in the Fabry-Perot cavity and to reduce the seed power in the slave diode. The seed beam then passes through a polarizing beam splitter (PBS) attached to a Faraday isolator (Qioptiq FI-680-5SV, -30 dB). A second PBS is passed which is rotated by 45° after the Faraday isolator. Inside the optical isolator, the Faraday effect makes the polarization of the light passing through rotate by 45° [Iiz02]. This setup ensures that no light is back-propagating to the seed laser diode but can pass through straight towards the output. The seed light passes through an additional fiber before being injected to the slave diode. The second fiber provides mode-matching of both beams, which is crucial for stable injection locking. The slave diode is placed in a collimation tube package (LT230P-B) in a temperature-controlled mount.

3 EXPERIMENTAL SETUP

In the collimation tube, a second Teflon ring of 1 mm thickness is present to put the laser diode further back for efficient collimation. A laser diode protection board is configured to the laser diode which consumes some 10 mA of current applied to the diode. For optimizing the fiber coupling, beam shaping optics are placed at the output of the slave diode. Beam shaping optics are not necessary for the Ushio diode in the second approach. The output of the diode after passing through the fiber and the isolator is split off for diagnostics and output. A small fraction is sent to the wavemeter and another small fraction is sent to the scanning Fabry-Perot cavity to beat with the seed laser. The free spectral range of the 10 cm long Fabry-Perot cavity is calculated to 1.5 GHz with eq. 2 and the finesse to a value of 21 with eq. 4. The finesse could have been further improved by changing the Fabry-Perot Cavity length. The spectrum of the transmitted signal of both beams can be observed with a photodiode at the same time or individually by blocking one of the beams.

3.2 Instrument control

Current modulation is introduced by an external modulation port of the laser diode current controller connected to the laser protection board. A Meerstetter TEC-1091 is employed in the setup for temperature control. There is a Python library available for the Meerstetter TEC interfacing via the USB port. After running the auto tuning in the Meerstetter TEC software, the appropriate PID-coefficients are found automatically. The target temperature can be set in a Python script by including the library. The type of temperature control can be chosen in the software which is either 'heat only' or 'Peltier element'. Voltage and current limitations can be set accordingly.

The laser diode involved in the first approach (Thorlabs) needs heating so that its frequency is close enough to the master laser frequency which is achieved by using a heating cartridge (HTW15W) with a $38\ \Omega$ resistance. Whereas the second laser diode (Ushio) is temperature controlled with a Peltier element (ETH-071-14-15). The object temperature is read with a $10\ k\Omega$ thermistor connected to the TEC.

At first, a laser diode controller Thorlabs LDC2000C is in use with a precision limited to 0.1 mA. Later, a Toptica controller is introduced which has a better precision. This is needed for setting the current precisely as the injection lock intervals can get very narrow and fall below 0.1 mA for high currents applied to the diode. Both controllers have a modulation input and a monitor connector. The monitor outputs are connected to the analog input ports of a LabjackBox T7. The modulation input is connected to a Digital-Analog Converter (DAC) port of the LabjackBox T7. The DAC can be set to values ranging from 0 to 5 V. There is a library (ljm) available for the LabjackBox to be Python controlled. In addition to the current readout, the analog input port of the LabjackBox can be used to read the power measured with a powermeter. The Oscilloscope TBS2000 shows the transmission signal of the Fabry-Perot cavity via a photodiode positioned behind the cavity and can be interfaced in python with the TEK VISA library. With this setup, fully automated measurements including temperature and current control, power and photodiode signal readout can be conducted. In addition, the wavelength of the master and slave beam can be checked with a wavemeter (High Finesse WS6-600).

4 Characterization of a 660 nm Thorlabs diode

The first approach included a diode with a typical center wavelength of 660 nm (Thorlabs L660P120). Maximal current through the diode is 210 mA and the absolute maximal output power is specified to 130 mW. As described in Section 2.1.1 the wavelength range over which a laser diode can be tuned depends on the band gap in use. For this diode, the maximal operating temperature is specified to be as high as 60 °C. The center wavelength is about 660 nm at room temperature and an injection current of 170 mA. Consequently, the high temperature end of the diode operating regime is interesting besides high injection current resulting in maximal output power. The diode is sold as single-mode in spatial mode.

At the outset, properties of the free-running diode such as the frequency dependence on different diode case temperatures, currents, and the lasing threshold are measured for the characterization of this diode in Section 4.1. The use of beam shaping optics and the resulting coupling efficiency are described in Section 4.2. In Section 4.3 the injection-locked state is demonstrated and characterized.

4.1 Free-running laser diode

Setting appropriate parameters for current and temperature through the diode in the free-running state is crucial for the diode to be injection locked. Hence, in the free-running state, the frequency dependence on different diode case temperatures and currents as well as the lasing threshold are abstracted. The master laser is blocked for the following measurements and they are done manually by setting a temperature and current through the diode.

4.1.1 Wavelength tuning

The wavelength of the diode as a function of the diode case temperature is shown in Fig. 5 a). In addition, the wavelength is observed when increasing the current to the maximal current value of 210 mA. This measurement is shown in Fig. 5 b).

Even though in general the wavelength increases with increasing temperature, the wavelength is quickly jumping between different values in the range of 668 to 688 nm at most temperatures and currents. The segments with constant wavelength over a temperature or current range are associated with one longitudinal mode. This phenomenon is known as mode hopping [WH91]. As a consequence of this, the current and temperature are adjusted accordingly to reach single-mode operation.

In Fig. 5 a) it is obvious that for this diode one can tune over a wide range of wavelengths. Even above the operation temperature, the wavelength is still tuned. Nonetheless, operating the diode above the maximal specified values probably has an impact on the diode lifetime. The wavelength tunes with temperature because both the optical path length of the cavity and the gain curve depend on temperature. The wavelength detuning has a different dependency on the optical path length and the gain curve, which results in wavelength steps in Fig. 5 a). This is associated with the tuning of one longitudinal cavity mode. Typical values for the wavelength steps are 0.4 nm. In the measurement shown in Fig. 5 a) some steps seem larger because there could be intermediate cavity modes missed in the manual measurements where a single-mode operation is obvious. However, sometimes laser diodes also jump over several longitudinal modes only to jump back at higher temperatures [WH91].

In Fig. 5 b) a similar curve is obtained by changing the injection current at a constant case temperature of 60 °C. Changing the injection current through the diode is thermally affecting the diode considering Joule heating. For this reason, most of the wavelength tuning characteristics are due to the change in carrier density in the junction changing the index of refraction. [WH91]

4 CHARACTERIZATION OF A 660 NM THORLABS DIODE

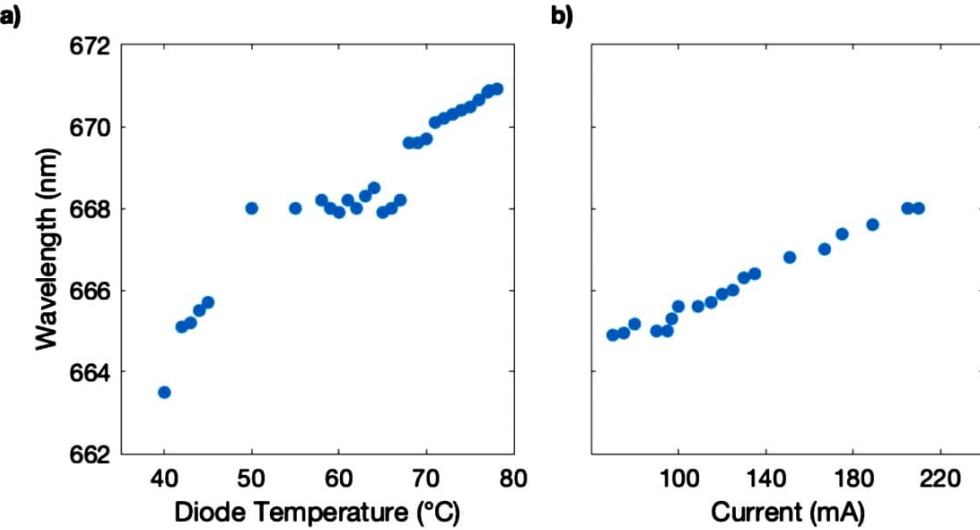


Figure 5: Measured wavelength as a function of **a)** slave diode case temperature at 210 mA slave current **b)** slave current at slave case temperature of 60 °C

4.1.2 Lasing threshold

The output power is measured right behind the diode at Point C indicated in Fig. 4 as a function of current through the diode at 77°C case temperature where a wavelength of just below 671 nm is observed and at 60 °C which is the maximal specified operational temperature. Together with the resulting linear fit, this is presented in Fig. 6. There is a sharp increase in the slope at (84.22 ± 0.02) mA for 77°C and at (78.89 ± 0.02) mA which results in a sudden onset of laser action. The errors on the lasing threshold are only derived from the linear fit. As follows in Section 4.3.2, the lasing threshold does not only change when a different case temperature is set to the diode but also when injection locking is present.

According to the datasheet, the maximal output power is 120 mW. This value is measured at 50 °C and below. When increasing the temperature further, the output power drops accordingly to a maximal value of 106.3 mW and 88.9 mW measured at 60 °C and 77 °C, respectively. Additionally, when increasing the temperature above the specified operating range, a "roll-over" in the output power due to heating of the diode is observed [Mes08].

4.2 Beam shaping

As discussed in Section 2.3.1, mode-matching of the injected seed beam and the slave laser diode beam is crucial for a successful injection lock. For this purpose, a single-mode fiber is employed between the optical isolator and the slave laser diode. The collimated slave laser diode beam needs to be circularized and expanded in diameter to increase the fiber coupling efficiency. Due to the rectangular shape of the gain region the output beam has an elliptical shape [WH91]. The beam is circularized by using cylindrical lenses with $f = -50$ mm and $f = 75$ mm. After the beam acquires a rounder shape, spherical lenses with $f = -100$ mm and $f = 150$ mm are employed to increase the beam size. Thus, it couples into the single-mode fiber with fiber couplers at both ends which take a beam waist that is slightly above 1.5 mm at best. The fiber coupling is improved at 60 °C and maximal current values after only a low fiber coupling efficiency resulted from coupling at a current just above the lasing threshold.

4 CHARACTERIZATION OF A 660 NM THORLABS DIODE

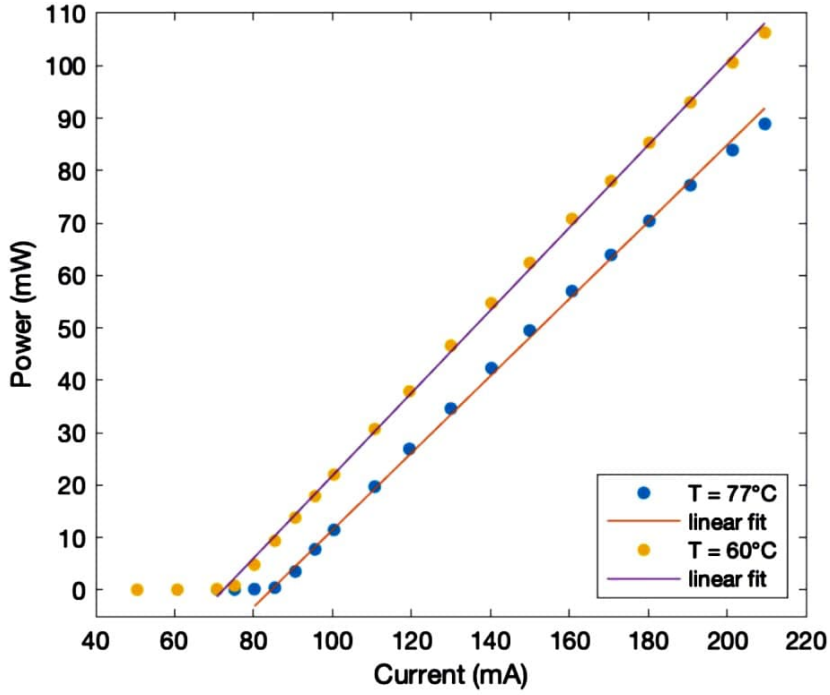


Figure 6: Measured output power at point C in Fig. 4 as a function of slave current at 21 °C case temperature

The combination of these telescopes results in a power efficiency through the single-mode fiber situated between points B and C in Fig. 4 of over 50 % for all currents through the diode but reaches values over 70 % for small currents as shown in Fig. 7 b). For higher temperatures, the fiber coupling efficiency and the slope of absolute output power decrease gradually as presented in Fig. 7 a). This behavior for higher currents might be due to different spatial modes appearing which are not coupled into the fiber. Still, using a different telescope and improving coupling through the fiber with different optical paths might improve the efficiency.

A glass plate aligned at the Brewster angle, which filters only for the horizontally polarized component of the beam, can be used to check the horizontal and vertical Gaussian beam diameter on the beam profiler. Additionally, a spherical lens with a focal length of 7.5 cm is introduced to focus the beam. The diameter of the seed and the diode laser beam can be checked to overlap well. The resulting Gaussian beam shape is shown in Fig. 8, where the $\frac{1}{e^2}$ -diameter of the transverse intensity profile is given in Eq. 15, is displayed as a function of the distance from the slave laser diode. In Fig. 8 a) the Gaussian beam shape is shown for a current value just above the lasing threshold at 90 mA and in Fig. 8 b) for the maximal injection current value of 210 mA. The values obtained at the focal point corresponding to the Gaussian beam diameter and the slope transferred to the half-angle divergence in front of the lens with eq. 18 are shown in Tab. 1.

At maximal current, the horizontal Gaussian beam diameter is more divergent than at lower currents. However, the measured Gaussian beam diameter at the focus of the lens is smaller at higher currents, whereas the divergence in the vertical axis reduces. This evolution in Gaussian beam parameters may cause the downturn of fiber coupling efficiency at high injection currents.

4 CHARACTERIZATION OF A 660 NM THORLABS DIODE

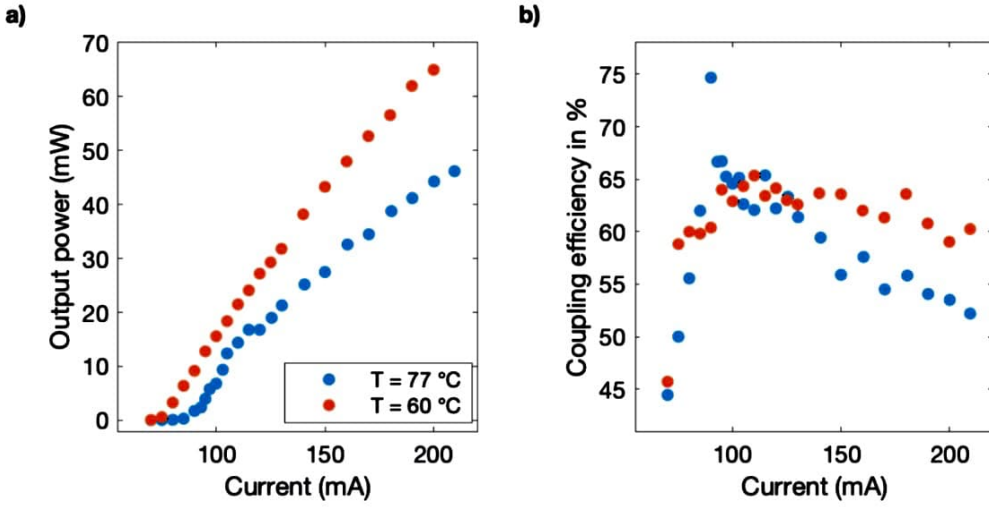


Figure 7: a) Output power measured at Point B in Fig. 4 and b) Coupling efficiency of the single-mode fiber between Point B and C in Fig. 4 as a function of slave current

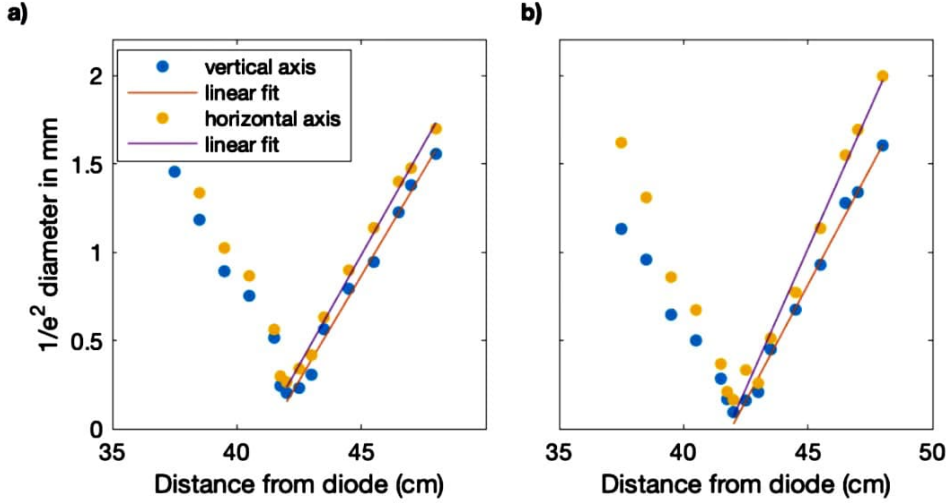


Figure 8: Beam shape with $60\text{ }^{\circ}\text{C}$ case temperature at a) 90 mA and b) 210 mA slave current

	w_0 (mm)	$\frac{\theta}{2}$ ($^{\circ}$)
Master laser vertical axis	0.063	0.669 ± 0.098
Master laser horizontal axis	0.065	0.760 ± 0.105
Slave diode vertical axis at 90 mA	0.203	1.719 ± 0.091
Slave diode horizontal axis at 90 mA	0.264	1.587 ± 0.119
Slave diode vertical axis at 210 mA	0.094	1.579 ± 0.110
Slave diode horizontal axis at 210 mA	0.164	1.946 ± 0.194

Table 1: Gaussian beam diameter and half-angle divergence of master and slave laser

4.3 Demonstration of injection locking

After ensuring mode-matching between the injected and the slave laser diode beam, making sure sufficient seed power is reaching the slave diode and making the slave laser diode run within the injection locking range frequency wise, one can demonstrate injection locking [SED19]. The injected seed power reaching the slave diode is 1.5 mW. At a preset constant temperature of 60 °C for the diode case, the current is slowly decreased to observe injection locking.

The main monitoring tools for observing injection locking are the transmission signal through the Fabry-Perot Cavity, the output power measured at point D in Fig. 4 and the monitoring photodiode signal of the slave laser diode situated behind the laser diode cavity (see Fig. 11). The photodiode current can be monitored with an oscilloscope by running it over a resistor. In this case, a $470\ \Omega$ resistor is in use.

Before conducting data for the current dependency of this diode, the measurement process was fully automated with the LabjackBox and the monitor and modulation ports of each instrument in use.

4.3.1 Current dependency

The following measurements for this diode have all been conducted with decreasing injection current through the slave diode. Compared to when the current would be increased, this results in a wider range of injection currents where the injection locking takes place [SPSG16]. The range of current where a stable injection lock is monitored is referred to as the injection lock width in the following. The details of the preferred decreasing current values are further detailed in Section 5.3.1. The demonstration of injection locking is mainly studied by changing injection current applied to the slave laser diode. The injection lock center, i.e., the mean value of the injection current through the slave diode where the injection lock is acquired and the value where it is lost, is shifted with changing temperature [SPSG16].

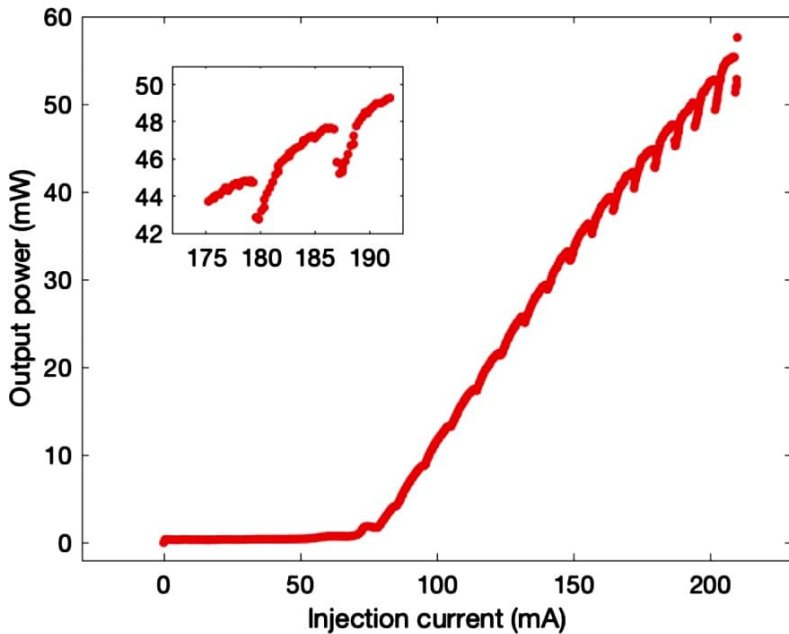


Figure 9: Power measured at point D in Fig. 4 as a function of slave current at 60 °C

4 CHARACTERIZATION OF A 660 NM THORLABS DIODE

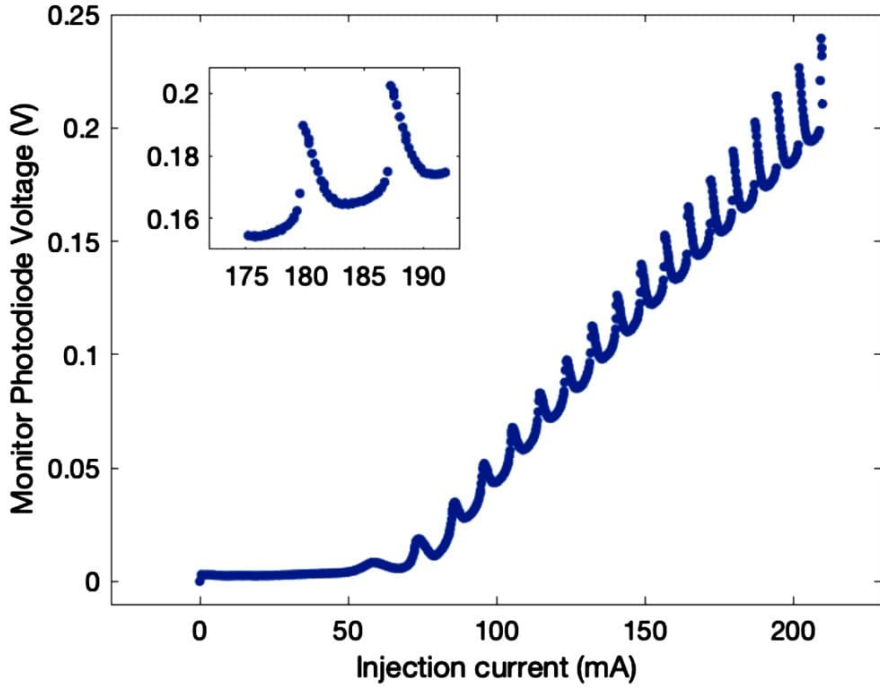


Figure 10: Slave diode monitoring photodiode signal situated behind the laser diode cavity (seed Fig. 11 as a function of slave current with 1.5 mW seed power at 60 °C case temperature

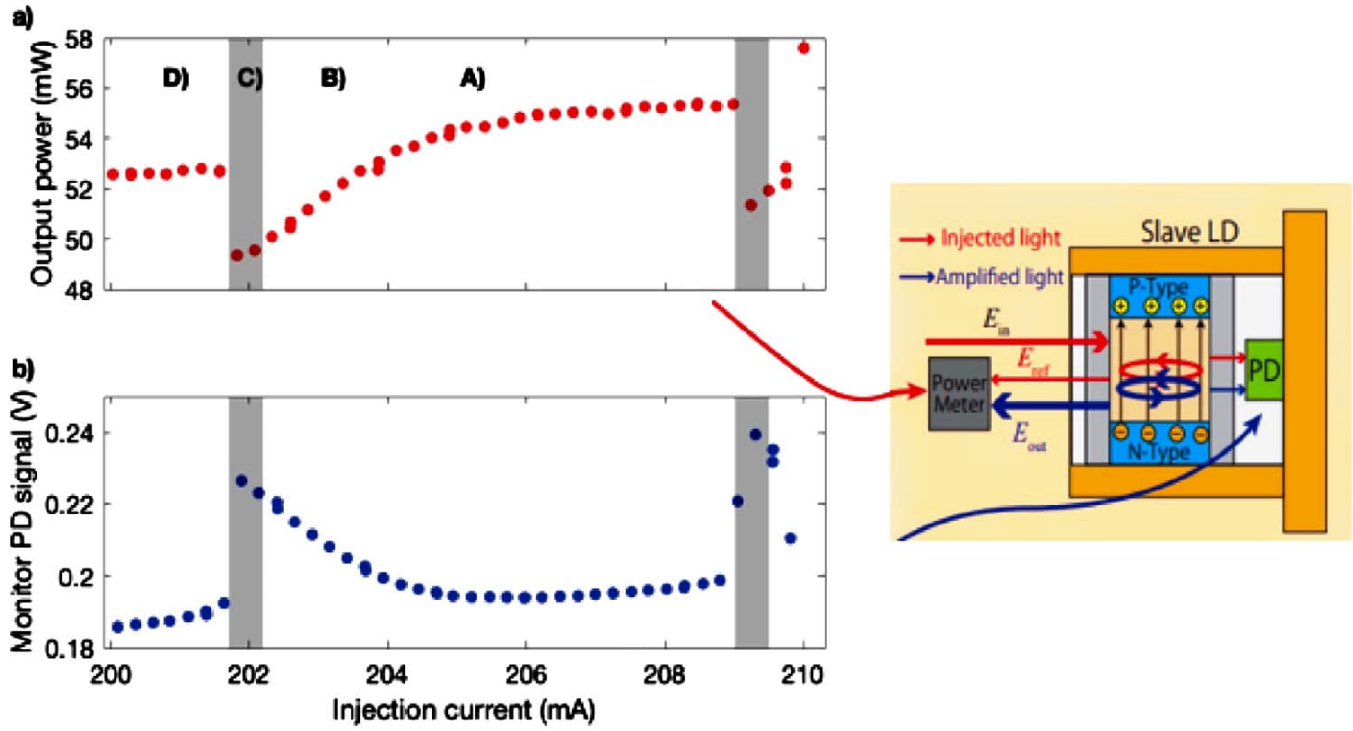


Figure 11: a) Output power measured at point D in Fig. 4 b) Monitor photodiode signal as a function of injection current at 60 °C and 1.5 mW seed power. Gray patches indicate single-mode areas in a) and b) where injection locking takes place. Schematics of Slave LD on the right taken from [HMIK15].

4 CHARACTERIZATION OF A 660 NM THORLABS DIODE

In Fig. 9 the variation in the output power of the slave diode measured at point D in Fig. 4 as a function of the slave injection current is shown. Likewise, the monitor photodiode signal of the slave diode as a function of the slave injection current is displayed in Fig. 10. In Fig. 11 a) the output power measurement from Fig. 9 and in Fig. 11 b) the monitor photodiode signal from Fig. 10 as a function of injection current in the range of 200 mA to 210 mA are displayed. The gray patches in Fig. 11 indicate the current interval where the slave laser diode is injection locked. These injection lock windows typically are on the order of 0.5 mA at 1.5 mW of injected seed power in this measurement. This injection lock interval can be identified with the transmission signal through the Fabry-Perot cavity of the slave laser diode in Fig. 12. Here, it is shown how the frequency spectrum from the Fabry-Perot cavity of the slave diode changes to a single sharp peak per free spectral range when decreasing the current. In Fig. 12 A) 202 mA and B) 201 mA are applied to the slave diode and no injection lock is observed. These current values correspond to regions A) and B) in Fig. 11. After all, there already is some coupling of the seed light to the cavity observed as there are single-mode peaks emerging, the output power is starting to decrease and the monitor photodiode signal is gradually increasing. The peak height of the Fabry-Perot cavity transmission signal of the slave diode can easily be compared to the peak height of the seed light passing through the Fabry-Perot cavity with the same intensity as the slave laser light. If the peak height of the slave diode matches the one of the seed light and the peak height of the transmission signal through the cavity, the slave diode light is fully single-mode. When the peak height of the slave diode is lower, only the fraction corresponding to the ratio of the slave diode peak height and the seed peak height is single-mode. The remaining part is keeping its broad spectrum [HMIK15]. This is why there are side maxima present in the transmission signal of the Fabry-Perot cavity in Fig. 12 A) and B).

The current can be decreased further until only single-mode peaks per free spectral range are observed and all side maxima of the slave diode are suppressed as shown in Fig. 12 C). This transmission signal is preserved for the whole injection lock window of 0.5 mA until the signal changes very rapidly when further decreasing the current. Fig. 12 D) shows the broad emission spectrum of the free-running diode in the Fabry-Perot cavity. Very weak or no coupling of the seed light to the cavity is observed. A discussion on the gradual increase in peak height when approaching the single-mode area from the high current end in comparison to the rapid decrease of the peak height accompanied by the loss of the injection lock is given in Section 5.3.1.

While the output power is decreasing when a single-mode area is approached, the monitor photodiode signal increases and reaches a maximal value. This is explained by the fact that negative interference occurs between the light from the slave diode output and the seeding light reflected at the front face of the diode [HMIK15]. At the same time, when the seed light couples to the cavity, the signal of the monitoring photodiode increases.

These single-mode areas with a stable injection lock appear periodically. They are separated by 7 mA of injection slave current. For verification that the periodicity in the injection current is associated with the free spectral range of the Fabry-Perot cavity of the slave laser diode, the frequency change of the laser diode output is measured at two different injection current values separated by a multiple of 7 mA. At 188 mA, a wavelength of 667.6 nm and at 97 mA a wavelength of 665.3 nm can be measured and 12 single mode areas are passed within this current range. Accordingly, the free spectral range is $\Delta\nu_{FSR} = 129.4$ GHz. With Eq. 1 and an estimate for the refractive index of $n \approx 1$ the cavity length then is given by roughly 1.2 mm. However, the refractive index in reality would be greater because the light passes through the semiconductor material. Thus, the cavity length is probably below 1 mm. Typical laser diode chip sizes are a few hundred micrometers [Sze81]. Therefore, the cavity formed in the laser diode in use for the injection lock is two mirrors on the front and back facet of the semiconductor.

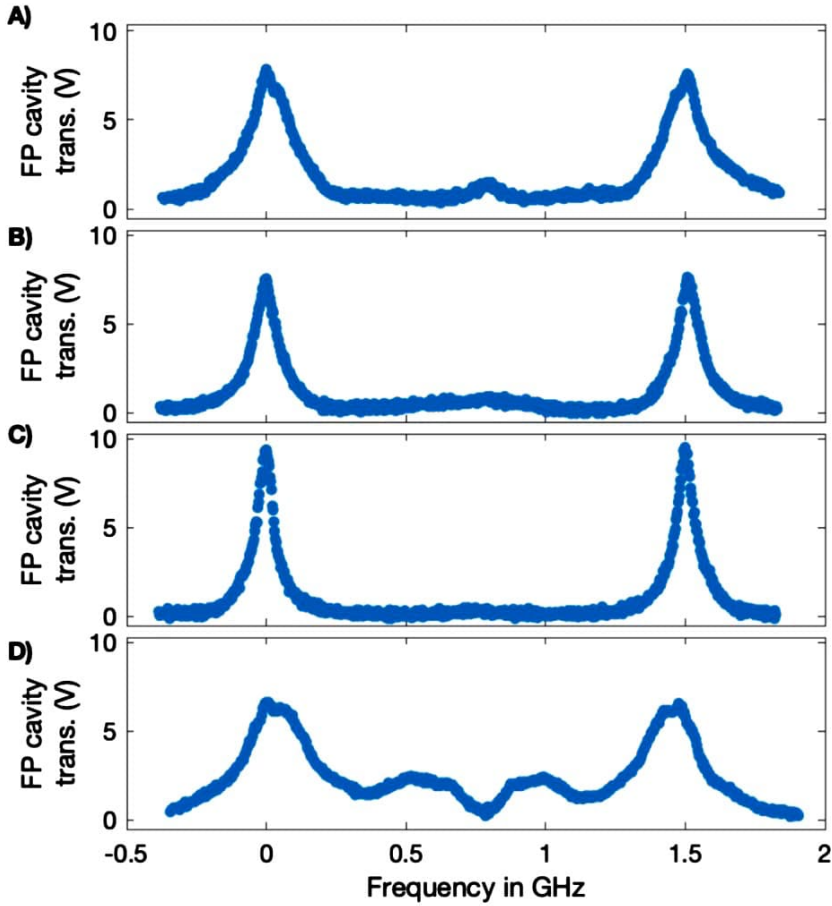


Figure 12: Fabry-Perot cavity transmission signal of the slave laser diode at 60 °C case temperature and 1.5 mW seed power with applied slave injection current values of **A)** 205 mA, **B)** 203 mA, **C)** 202 mA, **D)** 201 mA

4.3.2 Lasing threshold in injection locked state

With increasing seed power, the lasing threshold of the diode decreases. This behavior is discussed in [WYH⁺03]. Just above the lasing threshold, single-mode areas can be observed. In this way, the seed laser couples to the laser diode cavity, which results in sufficient gain through the laser diode for the lasing state to onset at lower current values.

The prediction of [WYH⁺03] could be experimentally verified by measuring the output power at point D in Fig. 4 as a function of the injection current through the slave diode. As this measurement pictured in Fig. 13 has been done manually, the measurement points only include the output power values at the selected injection current values and are not separated equally. In Table 2 the lasing thresholds for different values of seed power calculated with the linear fit of the values above the lasing threshold are displayed. The error is acquired from the linear fit and does not include an error from repeated measurements.

4 CHARACTERIZATION OF A 660 NM THORLABS DIODE

The bumps around the lasing threshold are due to the first injection locking range being visible in the jump of output power and are increased in intensity by the higher coupling efficiency at lower currents. Injection locking is observed for a seed power as low as 0.8 mW for all currents from 70 mA to 210 mA.

However, generally the injection lock quality is improving with increasing seed power. Thereby, the injection lock intervals get larger. This results in more stability over time. For the seed power of 0.6 mW, only the region around the lasing threshold is measured. The single-mode areas are vanishingly narrow for this value of injected seed power and are not displayed in Fig. 13. The overall output power does not reach the maximal value observed for this measurement because the coupling efficiency was improved after taking this measurement.

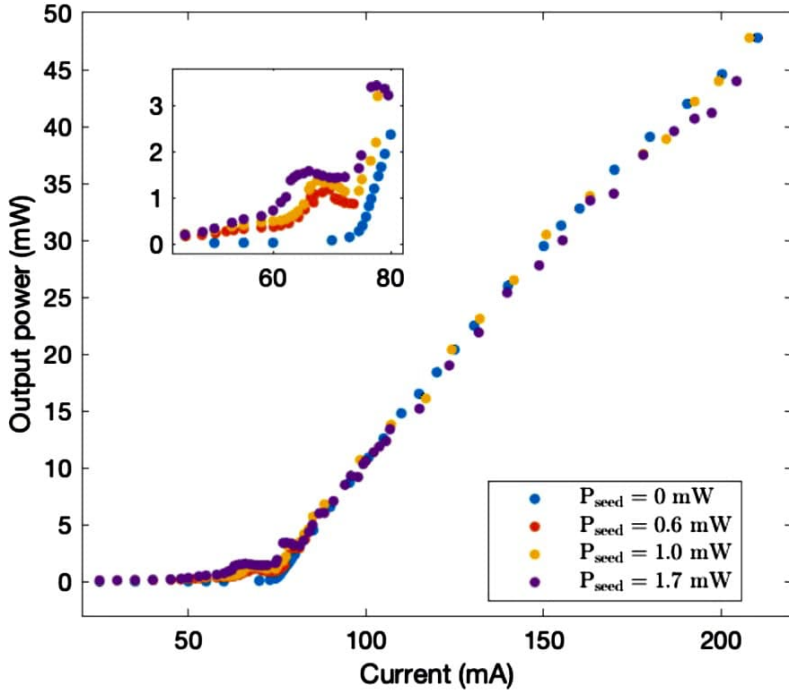


Figure 13: Output power measured at point D in Fig. 4 as a function of injection current for different seed power values injected to the slave diode

Seed power (mW)	Lasing threshold (mA)
0	75.20 ± 0.12
1.0	62.92 ± 0.19
1.7	61.28 ± 0.14

Table 2: Lasing thresholds for different seed power injected to the slave diode

5 Characterization of a 675 nm Ushio laser diode

The slave diode involved in the second approach can reach power values even above 0.2 W and works directly at 671 nm with appropriate current and temperature set. The maximal operational current of this diode is specified to 265 mA. It was initially expected that the diode needs some cooling to be close enough to the seed wavelength. Yet, the injection range is large enough to make the diode jump to the seed laser frequency even at 26 °C for all currents with 5 mW of seed power. The setup for this diode used a different seed laser, Li3, than in the first approach with Li2 in Section 4. Up to 5 mW of seed power are preserved at point C in Fig. 4.

The characterization of this diode follows the same structure as for the 660 nm diode starting with abstracting properties in the free-running state in Section 5.1 to ensure a resonance frequency close enough to the frequency of the injected seed beam. In Section 5.2 the fiber coupling efficiency is discussed. For this diode, the monitoring photodiode pin is not taken into use. Anyhow, the main monitoring tool for this diode is the automated acquisition of the single-mode peak height of the Fabry-Perot cavity transmission signal and again the output power. Thereby, it is possible to further analyze the dependence of stable injection lock quality on the seed power in Section 5.3.

5.1 Free running diode

5.1.1 Wavelength tuning

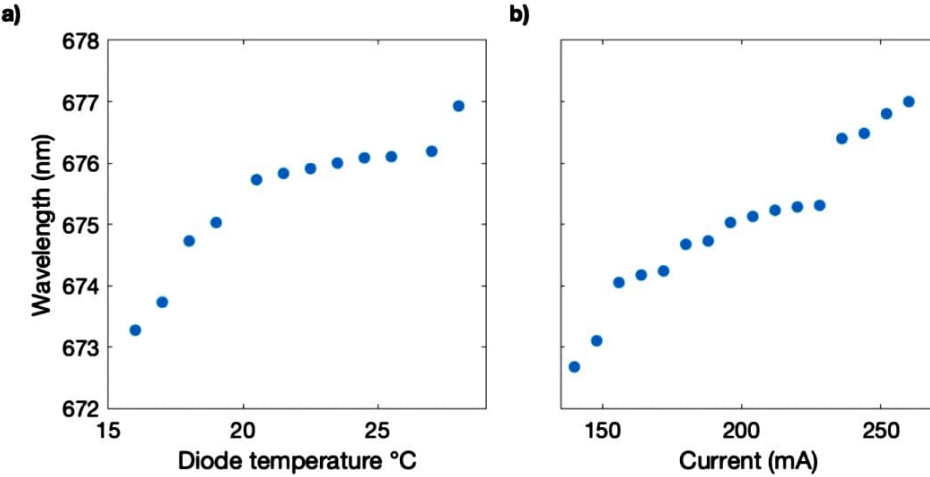


Figure 14: Measured wavelength as a function of a) slave diode case temperature at 265 mA slave current b) slave current at 20 °C diode case temperature

Fig. 14 reveals a similar relationship of the wavelength tuning as a function of slave diode temperature in a) and current in b) as for the 660 nm diode. Preferably, the diode could be run at 18 °C in the long run so that the frequency difference between the seed laser and the slave diode is less. This ensures more stable injection locking and still avoids condensation.

5.1.2 Lasing threshold

At a diode case temperature of 21 °C the output power measured at point C in Fig. 4 as a function of the applied current through the diode is displayed in Fig. 15. The lasing threshold is then determined to (50.666 ± 0.005) mA with a linear fit.

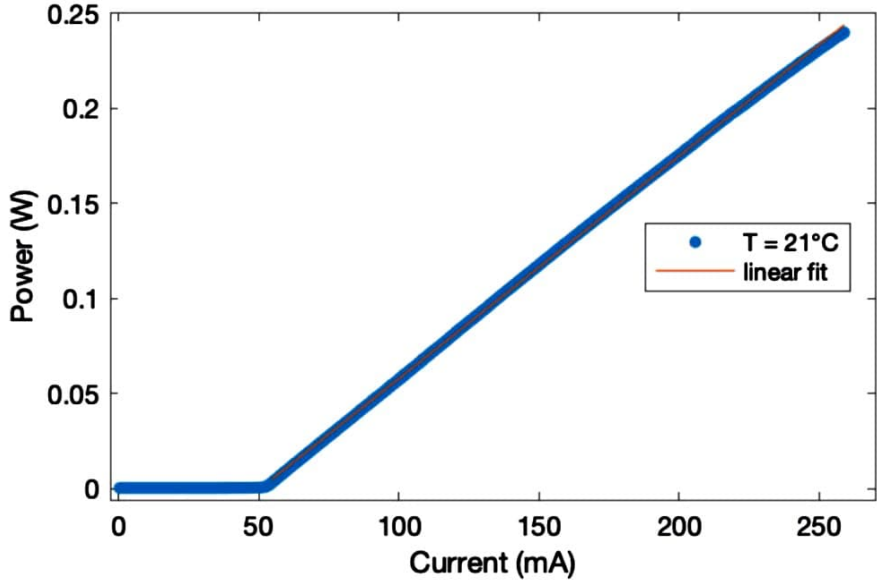


Figure 15: Output power as a function of slave injection current at a case temperature of 21° C

5.2 Beam shape and coupling efficiency

The coupling efficiency of the slave diode beam strongly depends on the case temperature and injection current. The output power measured as a function of the slave injection current at point B in Fig. 4 is shown in Fig. 16 a) for a set of case temperatures. The coupling efficiency is determined from the ratio of the power measured after the slave diode beam passed the fiber at point B in Fig. 4 and before passing the fiber at point C in Fig. 4 and the resulting values are shown in Fig. 16 b).

It was determined that between 20 °C and 22 °C the maximal output power values are achieved even though the coupling in the fiber has been optimized at 16 °C before. Coupling efficiencies with values above 50 % are reached for all currents above the lasing threshold. At current values above 240 mA, which lies above the operational current value of 230 mA, the coupling efficiency reduces or becomes constant. Below this, the coupling efficiency follows an upward trend with increasing current.

When fiber coupling at temperatures higher than 16 °C, the output power maximum measured afterwards is shifted further to higher temperatures. Shifting the maximum in output power to lower temperatures might be possible when changing the optical path from the slave laser diode to the fiber.

In the following measurements, the preset temperature value is held at 20 °C where the maximal fiber coupling efficiency and output power are detected after fiber coupling optimization at 16 °C. The beam shape at 200 mA and the maximal current of 265 mA are determined with a glass plate and a lens with a focal length of 7.5 cm and Eq. 18. The $\frac{1}{e^2}$ -diameter in the Gaussian intensity profile are pictured as a function of distance from the slave laser diode in Fig. 17. The resulting values for the Gaussian beam diameter and half-angle divergence are listed in Tab. 3. Although there are no beam shaping optics in use, the divergence in the vertical axis matches quite well with the one of the master laser. However, the beam size is larger in both vertical and horizontal directions. Apart from the different beam shapes, which did not exhibit a particularly Gaussian beam shape with the beam profiler, the coupling efficiency is sufficient to reach values of over 130 mW measured at the output indicated with D in Fig. 4.

5 CHARACTERIZATION OF A 675 NM USHIO LASER DIODE

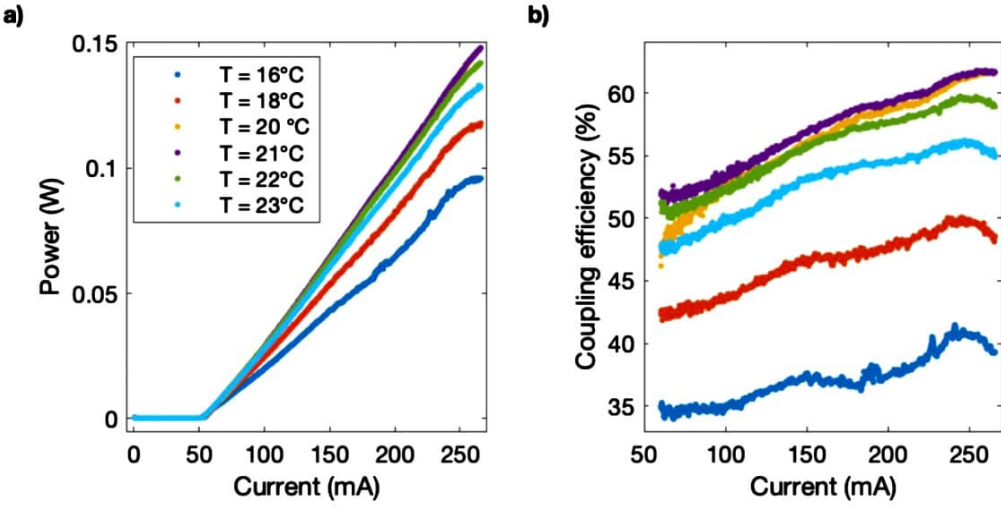


Figure 16: a) Output power measured after passing the fiber b) Coupling efficiency as a function of slave injection current for a set of case temperatures of the slave diode

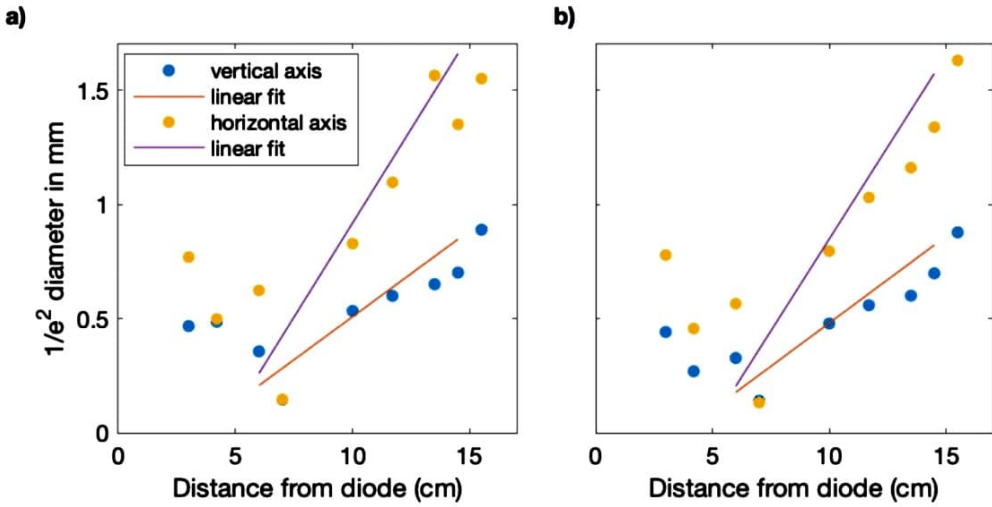


Figure 17: Beam shape at a) 200 mA b) 265 mA

	w_0 (mm)	$\frac{\theta}{2}$ (°)
Master laser vertical axis	0.074	0.665 ± 0.067
Master laser horizontal axis	0.073	0.749 ± 0.081
Slave diode vertical axis at 200 mA	0.144	0.668 ± 0.244
Slave diode horizontal axis at 200 mA	0.146	1.054 ± 0.374
Slave diode vertical axis at 265 mA	0.140	0.522 ± 0.168
Slave diode horizontal axis at 265 mA	0.132	1.008 ± 0.237

Table 3: Gaussian beam diameter and half-angle divergence of master and slave laser

5.3 Demonstration of injection locking

5.3.1 Current dependency

A similar behavior as for the 660nm Thorlabs diode in the first approach is observed in terms of the strong dependency on the slave current. In Fig. 18 the output power is measured as a function of decreasing as well as increasing injection current through the slave diode. The seed power is set to 5 mW and the case temperature to 20 °C. The single-mode areas for decreasing current and increasing current are marked with light and dark gray patches.

A significant difference can be found between the single-mode areas for increasing and decreasing current. When the current is increased, single-mode areas are shifted to higher current values and the current window is more narrow in comparison to when the current is decreased. The hysteresis behavior of an injection locked diode becomes obvious by this. In [SPSG16] this phenomenon is explained by the seed light being resonant with the slave diode cavity, resulting in a cavity expansion due to heating. When approaching a single-mode area from the low current side, there is no initial intra-cavity seed light which could drive the cavity expansion. Thus, the single-mode area is only reached at higher currents. To prevent a narrow injection lock width, it is beneficial to reach single-mode areas by decreasing the current through the slave diode! Here, the periodicity of the injection current is about 8 mA. For this diode, the association with the free spectral range is verified as well. Accordingly, the free spectral range is calculated to $\Delta\nu_{\text{FSR},\text{LD}} = 115.2 \text{ GHz}$ with values from measuring the frequency of the free-running slave diode at two different current values over the range of 8 single-mode areas. The slave diode cavity length is then determined to $L \approx 1.3 \text{ mm}$ with eq. 1. The refractive index is again approximated to $n \approx 1$.

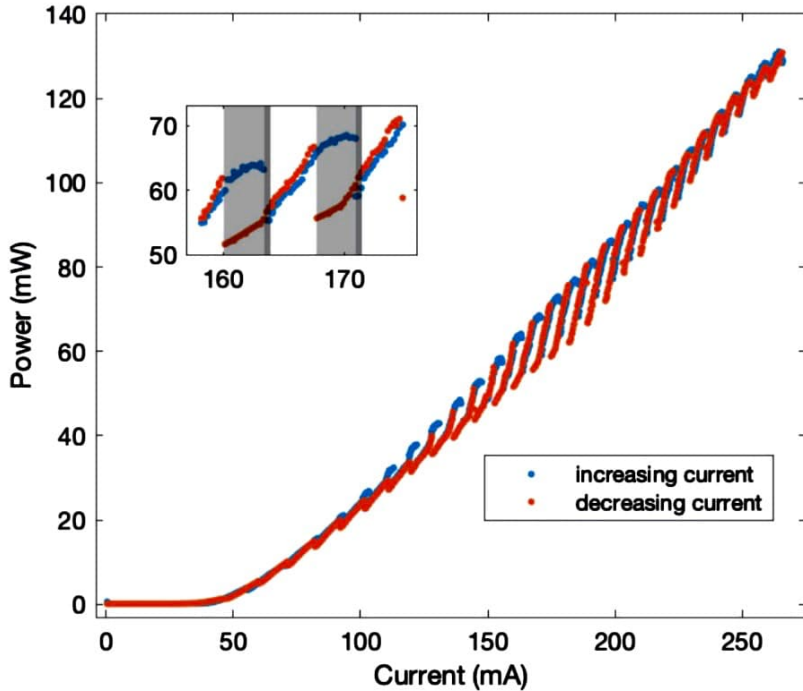


Figure 18: Output power measured at point D in Fig. 4 as a function of slave current. Light gray patches indicate single-mode areas for decreasing and dark gray patches for increasing current.

5 CHARACTERIZATION OF A 675 NM USHIO LASER DIODE

In Fig. 20 the change of the Fabry-Perot cavity transmission signal of the slave diode is shown for decreasing current values. Even though single-mode areas can be identified with the output power response as a function of both increasing and decreasing current as displayed in Fig. 19 a), one can fully characterize them with a "spectral purity curve" [SPSG16] which is shown in Fig. 19 b). The spectral purity curve can solely be conducted from a measurement collecting the peak height of the transmission signal of a Fabry-Perot cavity, when the slave diode beam is fed into the cavity, with decreasing current. There is no need to acquire the same curve for increasing current. This also allows to monitor the injection lock quality in terms of the locking window only while decreasing the current. Due to the sudden loss of injection locking on the low-current side of the injection lock window indicated in part C of Fig. 19 b) in comparison with the gradual increase in peak height shown in part A of Fig. 19 b) spectral purity curves are asymmetric [SPSG16]. There is strong coupling observed on the high current side of the a spectral purity curve when a single-mode peak emerges in the Fabry-Perot cavity transmission signal. This can be verified in Fig. 20 A). Still, this is only partially single-mode as described above unless the maximal value of peak height is reached. This value remains constant over the whole injection lock interval. The flat plateau from 182 mA to 184.5 mA in part B of Fig. 19 b) presents the injection lock interval. The transmission signal in Fig. 20 B) is comprised of the single-mode peak. Decreasing the current further leads to a rapid loss of the injection lock. Then a broad emission spectrum, indicated in Part C of Fig. 19 b) and Fig. 20 c), can be observed.

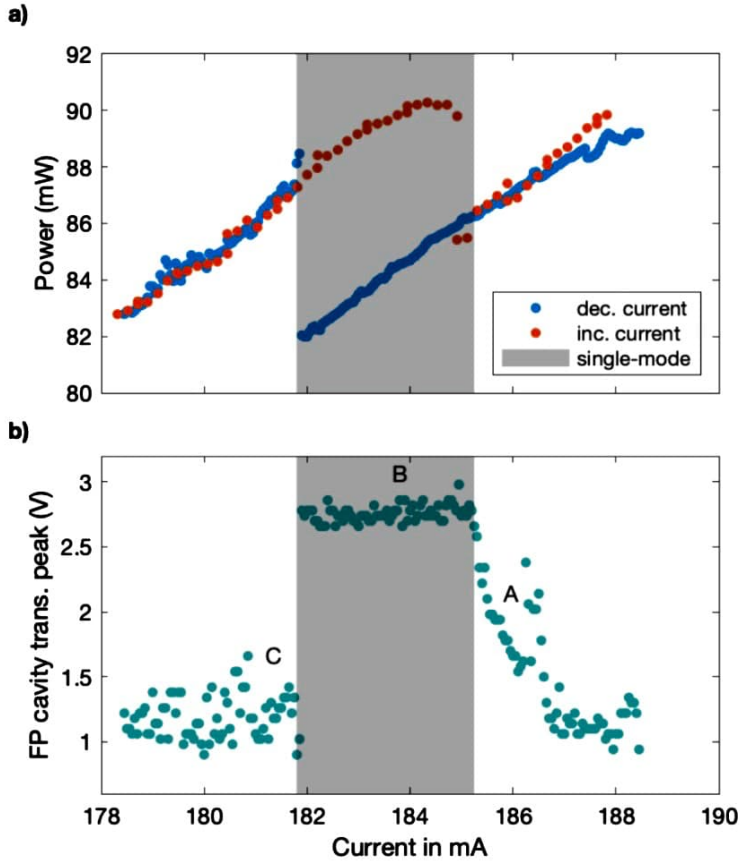


Figure 19: a) Power (point D in Fig. 4) b) spectral purity curve as a function of slave current

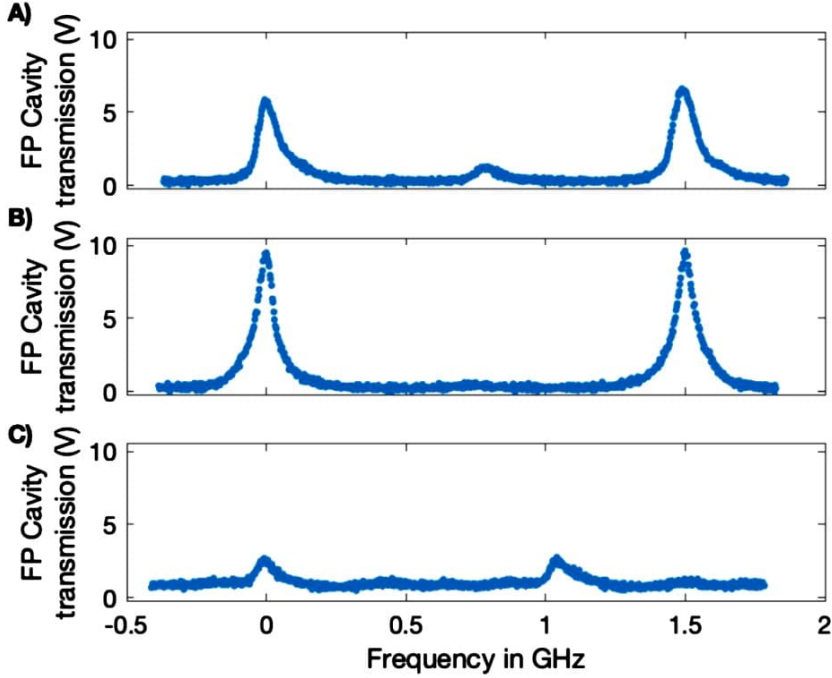


Figure 20: Fabry-Perot cavity transmission signal of the slave diode at **A)** 186 mA, **B)** 184 mA, **C)** 181 mA applied to the slave diode

In [SPSG16] the asymmetric nature of spectral purity curves are detailed further: There are two thermal effects playing a role in the slave diode. One is caused by Joule heating from the current through the diode and the other by heating from the seed light being resonant with the slave diode cavity. When decreasing current from the high-current end of the spectral purity curve, the cavity is shortened due to a decrease in Joule heating. At the same time, the cavity is expanded due to the seed light being resonant with the cavity as it approaches the flat plateau where a single-mode area is obtained and the seed light is completely resonant. The seed light being resonant with the slave diode cavity is associated with heating and this leads to the expansion acting against the reduction in cavity length. On the other hand, when reducing the current further, these two effects do not compete anymore, but act with each other. This is due to the fact that the seed light is not resonant with the cavity anymore. Thus, it is shortened further leading to the very rapid change in the peak transmission signal.

5.3.2 Current-temperature stability maps

To run a stable injection lock, the current and temperature need to be adjusted at the slave diode to reach a single-mode area. As described above, these areas can be characterized with the output power and spectral purity curve obtained from the slave spectrum measured with the Fabry-Perot cavity. A Python script is written to obtain current-temperature stability maps [Ade19]. The temperature ranges from 19 °C to 22 °C in steps of 0.005 °C. In between these steps, the script pauses for 15 s to allow the temperature to be stabilized. Afterwards, the current is tuned from 160 to 265 mA in 0.2 mA steps while the output power and spectral purity curve are measured. Fig. 21 shows the acquired data for one preset temperature value of 19.505 °C. The injected seed power is 4 mW throughout all measurements for the current-stability maps.

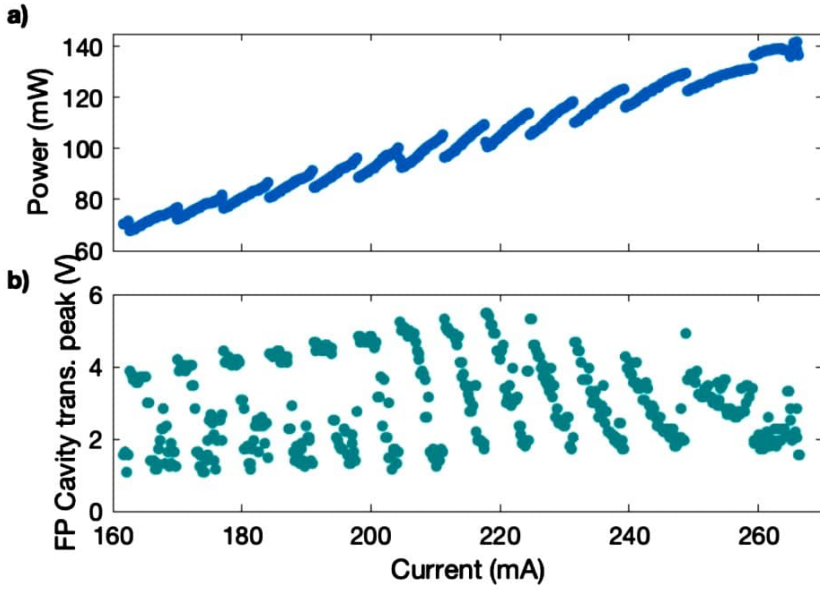


Figure 21: a) Output power measured at point D in Fig. 4 b) Fabry-Perot cavity peak height as a function of slave injection current at 19.505 °C slave diode case temperature

In Fig. 22 a), c) each point of temperature and current is color coded with the peak height of the corresponding spectral purity curve. Whereas in Fig. 22 b), d) the data points are color coded with the measured output power values. Top row shows the acquired data for decreasing current and the bottom row for increasing current values. All maps exhibit that temperature shifts the whole spectrum strongly depending on the set current through the slave diode. The single-mode areas are indicated by constant output power and peak height over an evolution in the injection current. On the low current side, the signals undergo a rapid change. It can be verified that single-mode areas are evenly spaced and separated by higher values of output power in Fig. 22 b), d) and smaller values of peak height in Fig. 22 a), c). The gradual decrease in output power and an increase in the transmission signal peak height are detected on the high current side of each single-mode area.

Although single-mode areas seem to be existent above the operational current as well, they could not be investigated over longer timeframes in the slave spectrum measured with the Fabry-Perot cavity. This indicates that either the injection lock window is below the current step size 0.2 mA or coupling of the seed light to the slave laser diode is not sufficient. Or the frequency might be out of the locking range at high currents.

Around 19.5 °C single-mode areas with a high quality injection lock can be identified in Fig. 22 a) when the current is decreased. Here, very high peak heights in the Fabry-Perot transmission signal are encountered, even just below the operational current of 230 mA.

Between 245 mA and 265 mA, the output power increases in a very narrow current range for both decreasing and increasing current. However, unexpected behavior ensues at high currents when decreasing the current as seen in Fig. 22 a) and b). The contrast lines indicating single-mode areas increase in slope instead of decreasing.

5 CHARACTERIZATION OF A 675 NM USHIO LASER DIODE

The same behavior is observed with single-mode areas appearing periodically in Fig. 22 c) and d). Interestingly, the unexpected shapes of the single-mode areas are not present when increasing the current. Through to the maximum current, there are roughly evenly spaced single-mode areas with a falling slope. Both for increasing and decreasing current, the measurements are repeated for lower seed powers and the unexpected behavior at high currents when scanning the injection current from higher to lower values is present throughout all measurements. The reason for this remains unclear.

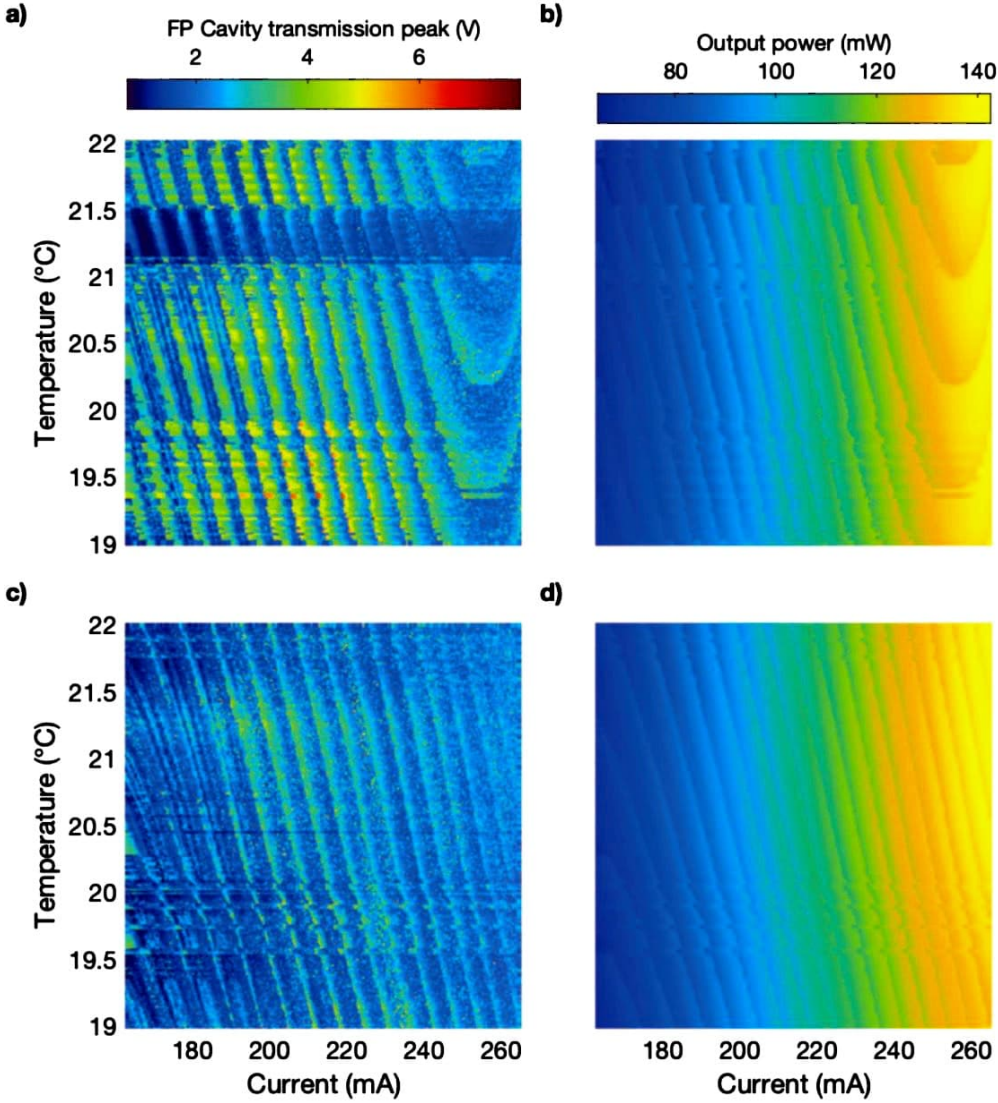


Figure 22: In the top row are current-temperature stability maps for decreasing slave diode current and slave diode case temperature and bottom row for increasing slave diode current and case temperature with color coding corresponding to a), c) Fabry-Perot transmission peak height of slave diode and b), c) output power measured at point D in Fig. 4 with 4 mW of injected seed power

5.3.3 Lasing threshold in injection locked state and variation of seed power

For the Ushio diode, a shift to lower currents of the laser threshold in the injection locked state is seen in Fig. 23 as well as for the Thorlabs diode. The corresponding values for the lasing threshold are listed in Tab. 4. At the same time, the inclines in output power get larger for higher values of seed power. As for the 660 nm Thorlabs diode, this is due to a stronger coupling and the resulting negative interference between the seed light reflected from the front facet and the amplified light from the slave diode [HMIK15]. Additionally, the jumps indicating the loss of an injection lock get very small and the slope of the output power incline is reduced around the lasing threshold. This behavior speaks for a continuous injection lock achievable with sufficient seed power on the order of over 10 mW [MOJ85]. Further discussion on the impact of seed power on the quality of an injection lock is provided in Section 5.3.4.

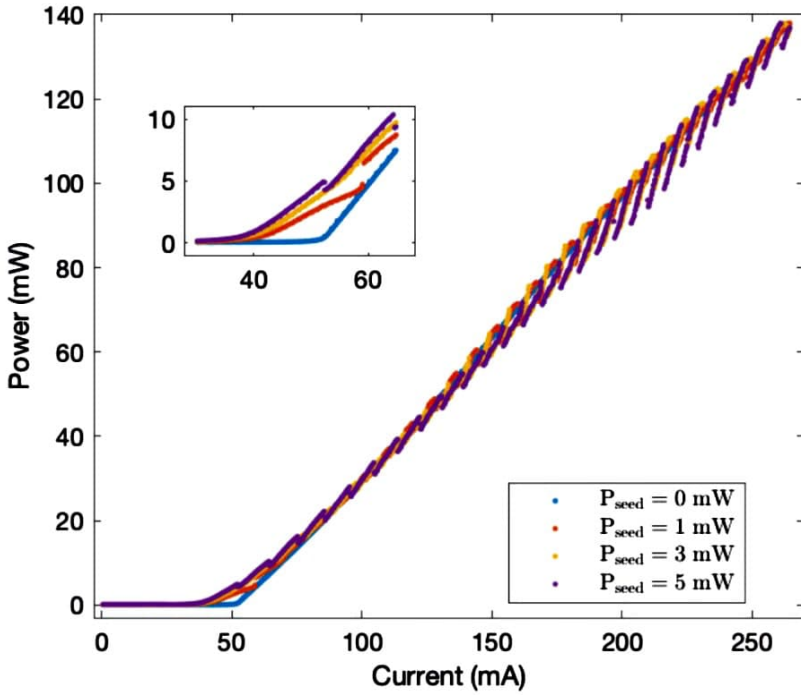


Figure 23: Output power measured at point D in Fig. 4 as a function of slave current for seed power values between 0 and 5 mW

Seed power (mW)	Lasing threshold (mA)
0	50.66 ± 0.01
1	42.81 ± 0.08
3	42.01 ± 0.08
5	41.89 ± 0.19

Table 4: Lasing threshold for a variation of seed power

5.3.4 Minimizing seed power

As described above, the spectral purity curve allows to measure the injection lock width while scanning through the slave current from high to low current values. There is no need to repeat the measurement while increasing the slave current to identify single-mode areas. For these measurements, the Toptica current controller is set up because it has a higher resolution and precision of below 0.1 mA when setting the range appropriately. Slave current is decreased in 0.01 mA steps and seed power from 4 to 1 mW.

In Fig. 24 the measurement is conducted for a single-mode area just above 180 mA. The same measurement is repeated for a single-mode area situated just below the operational current of 230 mA and the results are displayed in Fig. 25.

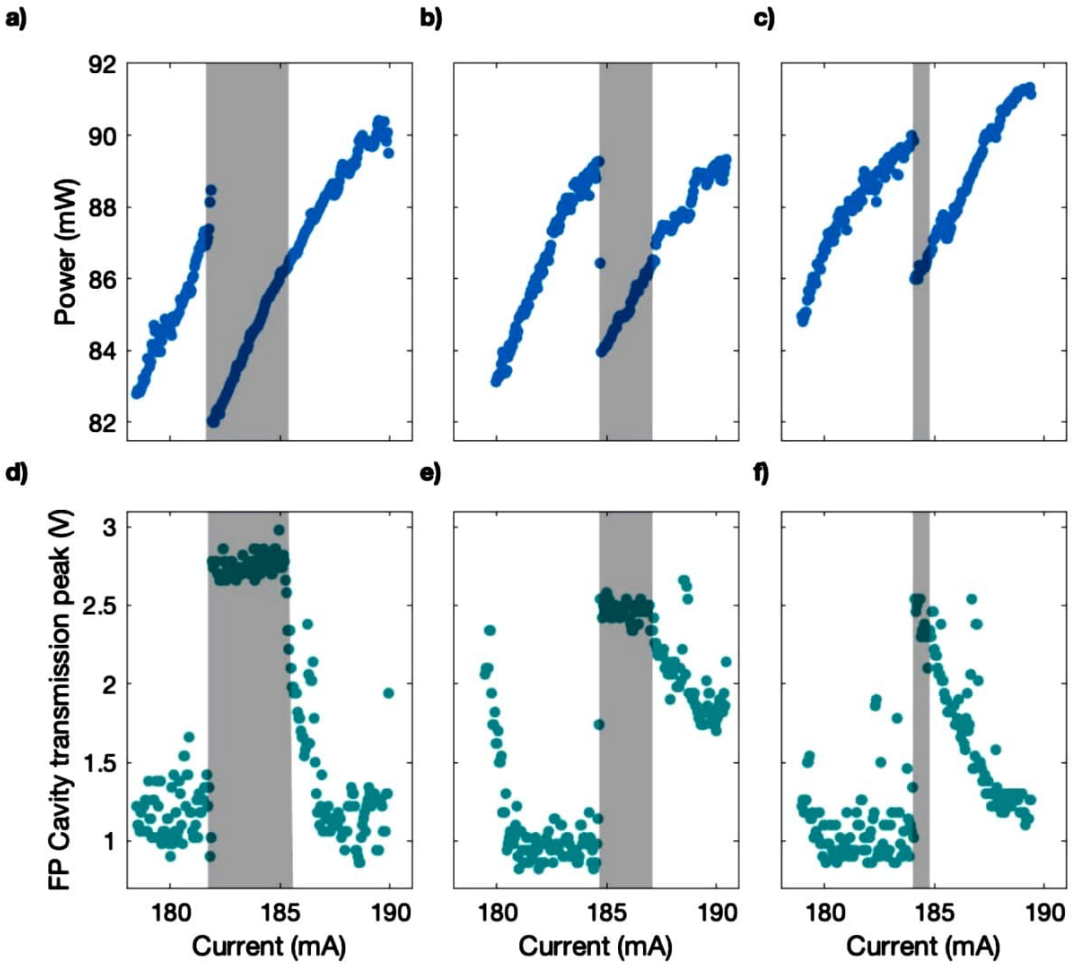


Figure 24: Top row is output power measured at point D in Fig. 4 and bottom row is the spectral purity curve of the slave diode for seed power of a), d) 4 mW, b), e) 2 mW and c), f) 1 mW at slave current above 180 mA

5 CHARACTERIZATION OF A 675 NM USHIO LASER DIODE

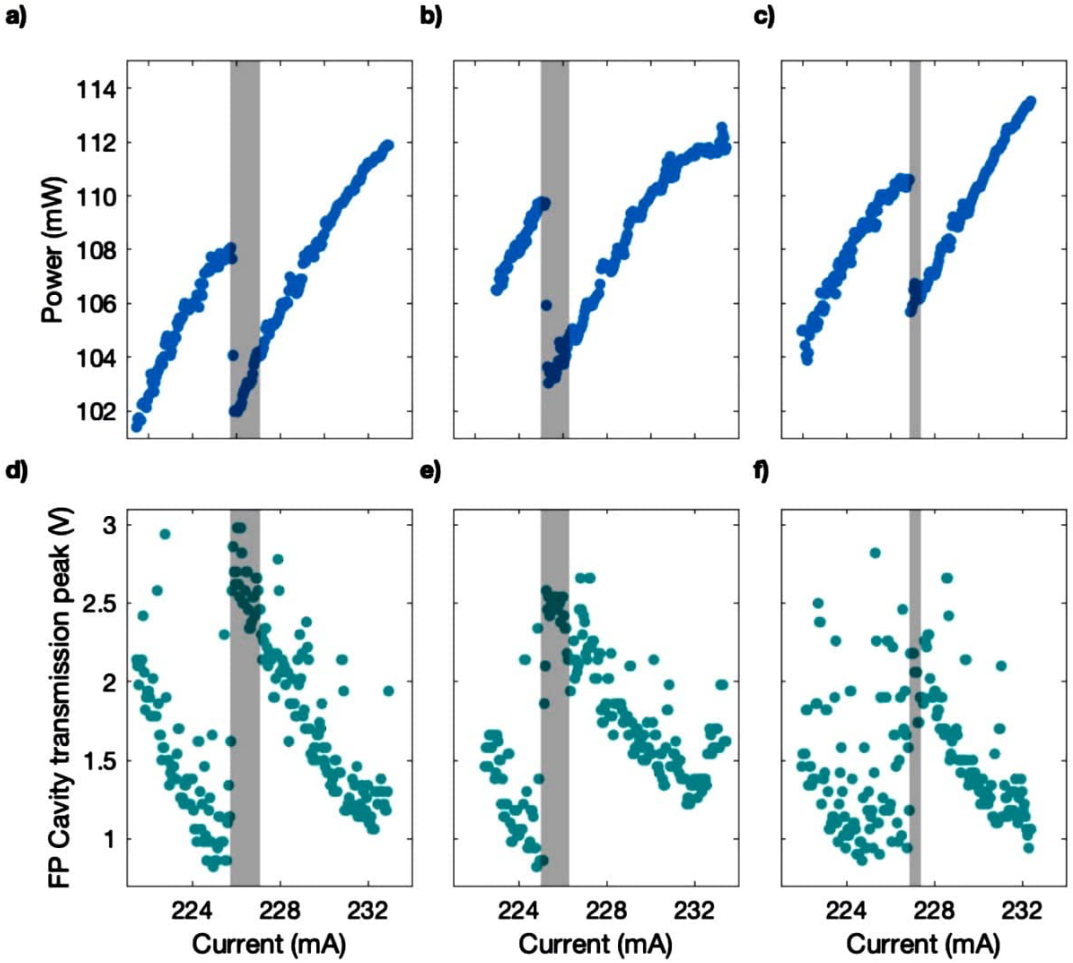


Figure 25: Top row is output power measured at point D in Fig. 4 and bottom row is the spectral purity of the slave diode for seed power of a), d) 4 mW, b), e) 2 mW and c), f) 1 mW at slave current above 220 mA

It is clear that the injection lock interval gets smaller by varying the seed light power to lower values. Additionally, the peak heights of the transmission signal through the Fabry-Perot cavity in Fig. 24 and 25 d), e) and f) decrease and the output values in Fig. 24 and 25 a), b) and c) do not decrease as much when approaching a single-mode area. This stems from the fact that not all light is fully single-mode but a fraction of the slave diode output keeps its broad emission spectrum. This phenomenon is observed more frequently at higher current values where the injection lock windows get narrower. These windows might be smaller than the resolution of the current controller which fails to set a current value within the injection lock range. Most of the slave diode light stays broad emission above the operational current although there is at least injection pulling identified as it becomes clear in the current-temperature stability maps in Fig. 22.

5 CHARACTERIZATION OF A 675 NM USHIO LASER DIODE

In Fig. 26 a) and b) the injection lock interval width as a function of seed power is shown for slave diode current values just above 180 mA and above 220 mA. The injection lock width for this measurement is defined by a threshold value. This threshold can be acquired from the minimal value in the flat plateau region. The signal-to-noise ratio has not been taken into account. The minimal width recognized at just above 186 mA is 0.1 mA and 0.02 mA at 220 mA with injected seed light of 0.5 mW, respectively. As can be seen from this figure, the injection lock width decreases strongly when the seed power is decreased. Steps in this downward trend can be observed as suggested in [SPSG16].

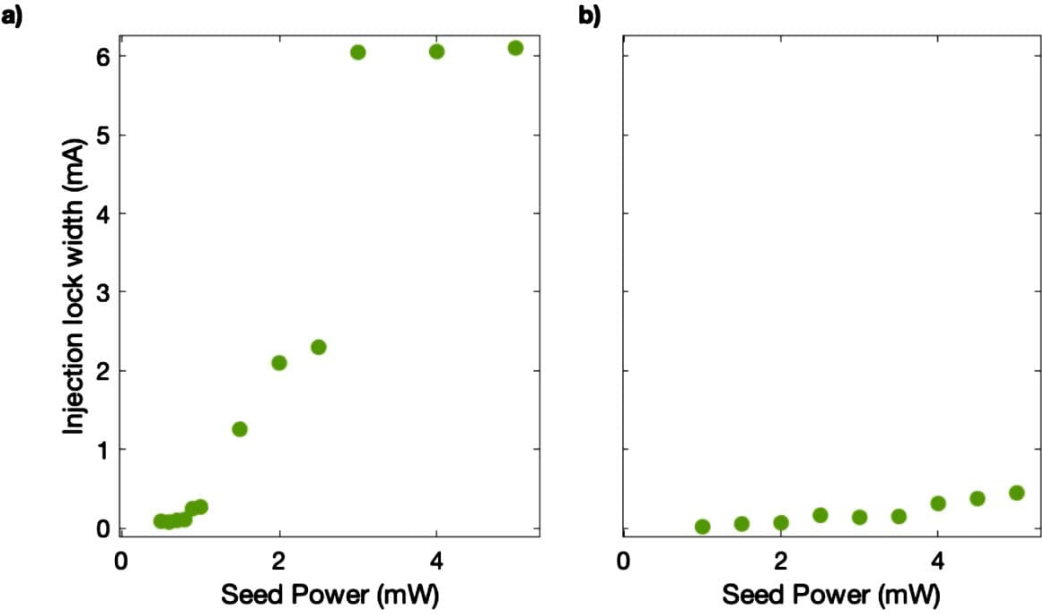


Figure 26: Injection lock width from spectral purity curves of the slave diode at slave current of a) 186 mA b) 225 mA

In the following, an estimation of the required seed power to get into a continuous injection locking range over all currents is attempted and based on [MOJ85]. With the estimation of the slave diode cavity length, it is possible to give an estimate of the injection locking range for this diode with eq. 10. By putting the injection efficiency $\eta \approx 1$, the line width enhancement $\alpha \approx 3 - 50$, the refractive index $n \approx 1$, the free spectral range $\Delta\nu_{\text{FSR}} = 115.2$ GHz, injection seed power $P_i = 1$ mW and slave diode output power $P_0 = 240$ mW the calculated locking range is $\Delta\omega_{\text{lock}} \approx 41 - 647$ GHz depending on the line width enhancement factor α intrinsic to the semiconductor material in the slave diode. However, e.g. for $P_i \approx 1$ mW the injection lock range must be below the value of the free spectral range of the laser diode cavity. Otherwise, there would be a continuous locking range over all currents expected [MOJ85]. In such a way the line width enhancement factor is approximated with $\alpha \approx 3$. By rearranging eq. 10 an estimation for P_i overcoming the free spectral range of the slave laser diode $\Delta\nu_{\text{FSR}}$ can be given. Then P_i is estimated to 24 mW to achieve a continuous injection locking range over all injection currents. The estimated value for P_i reduces significantly if α is set to a higher value.

6 Active stabilization of injection locking

Seed light power is valuable throughout the entire experiment. Hence, it is preferable to further reduce the seed light power. On the other hand, further decreasing seed power results in a smaller injection lock interval as seen in section 5.3.4. This can lead to a loss of injection lock after some time caused by thermal or mechanical disturbances such as drifts in the current or temperature. This can be avoided by using a higher value of seed power so that the injection lock interval gets larger and possible current and temperature drifts lie within this interval. This is referred to as a passive approach to stabilizing an injection lock. When actively stabilizing the injection lock rather than setting a current value manually, the seed power level is expected to be reduced by a factor of three. The following outline of active stabilization of the injection lock is based on [SPSG16].

A lock servo is in use for the implementation of active stabilization. This makes use of the spectral purity curve and keeps the current set to a value on the high current end of the plateau region marked with a yellow patch in Fig. 27. The injection locked state is defined by the threshold of 95 % of the peak height of the transmission signal through the Fabry-Perot cavity of the slave laser diode measured over the last passed second.

There are two modes implemented in the lock servo which run depending on the peak height being above or below the defined threshold value. If the peak height is above the threshold, the recovery program runs. The current is adjusted at higher currents in 0.1 mA steps until the threshold is reached. Then the active servo mode is activated and runs every 2.5 seconds. In this mode, the current through the diode is set to a value on the high-current side of the plateau region of the spectral purity curve to avoid a sudden change in peak height, resulting in the loss of the lock. This is done by measuring the current values at $i \pm \delta$ where i is the current set value. Slight changes in this offset current are detected and if $i + \delta$ is no more than $p1$ % below the peak measured at i the current is set to the offset value. On the other current side, if the peak height at $i - \delta$ is increasing by more than $p2$ % the new set current is this offset value. The values in use for δ , $p1$ and $p2$ can be adjusted depending on the noise signal of the plateau region. The peak height at one set current value can be measured and stored over a few free spectral ranges. In comparison to [SPSG16], the active servo mode has been tested with a Labjackbox and an oscilloscope output instead of an Arduino. An injection lock at 211 mA could be preserved over an hour with just 1.5 mW of seed light power reaching the USHIO diode. Further optimization of the parameters and the use of a cost-effective Arduino is needed to make this approach scalable.

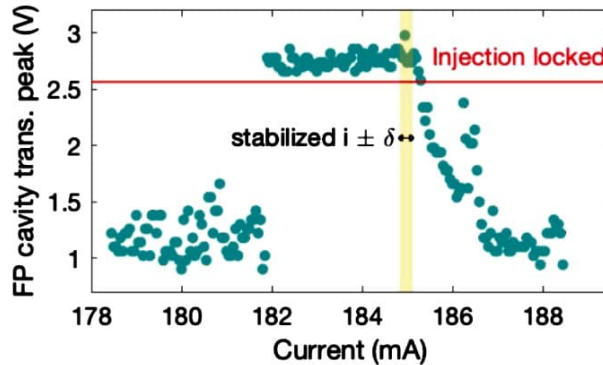


Figure 27: Spectral purity curve from Fabry-Perot transmission signal peak as a function of slave injection current with indicated actively stabilized injection current and threshold for the injection locked state

7 Conclusion

Sufficient output power of over 100 mW is achieved with the Ushio diode after employing both diodes in the injection lock setup. The use of the Ushio diode is determined to be more scalable in comparison to the Thorlabs diode. It can be injection locked close to room temperature at 20 °C. The output power is already twice the amount of the Thorlabs diode in the free-running state. Additionally, sufficient fiber coupling of over 50 % is achieved for all injection currents without any beam shaping optics in use.

The setup can be further improved by optimizing the fiber coupling efficiency at lower temperatures. This could be done by changing the optical path from the slave laser diode to the single-mode fiber. It is favorable to have the maximum output power at 18 °C to keep the frequency difference between the seed and slave diode laser to its minimum while staying above the dew point. Keeping the frequency difference between the seed and slave diode laser to its minimum is beneficial in terms of stability. The capturing range for injection locking is observed to be as high as 4 nm at its maximum. Higher differences in wavelength only result in some coupling between the seed beam and the slave diode cavity, but single-mode areas cannot be achieved. This is probably seen above the operational current through the Ushio diode, in which the resonance of the slave diode cavity is detuned too far from the master laser frequency.

Additionally, maximizing the efficiency through the Faraday rotator results in higher output power. While the maximum efficiency is observed through the Faraday rotator of 95%, only 89% is achieved during the measurements with the Ushio diode.

Mode-matching of the master laser beam and the slave diode beam is ensured by using a single-mode fiber in the setup. Robust injection locking could only be observed with the introduction of a single-mode fiber. In terms of robustness, it is important to reach the single-mode areas of injection locking from the high injection current end. This not only widens the injection lock widths in current tremendously but makes the locking more stable over a long period of time [SPSG16].

Operating the Ushio diode above the operational current of 230 mA results in unexpected behavior and makes a stable injection lock impossible even though there can be strong coupling observed. Even just below the operational current, the injection lock window is very narrow and on the order of 0.1 mA for typical seed power values of 5 mW. This shows how trading output power against injection lock stability is inevitable.

However, techniques for active stabilization of injection locking, as discussed in Section 6, allow for lower values of seed power injected to the slave diode. Such automatic lock schemes show promising results over long periods of time.

When passively stabilizing the injection lock, there is a need of keeping the seed power to values of above 5 mW to ensure the diode stays locked over a long time and producing sufficient output power of values above 100 mW. An approach to achieve much higher values of seed power would be: Setting up one injection locked Ushio diode at an injection current of e.g. 180 mA which results in a very wide single-mode area and an usable output power of above 80 mW. This in turn could be used as the seed light injected into several slave diodes. With achievable seed power values of more than 20 mW for one slave diode, continuous injection locking, where the current does not have to be adjusted to reach single-mode areas, might get observable [SED19]. Then, the locking bandwidth exceeds the value of one free spectral range of the slave diode laser cavity. This results in a large range of currents where no unlocking is apparent. From a practical point of view, this could be very useful in large-scale cold atom experiments with numerous components, which need to be relied upon.

References

- [Ade19] ADEMA, Joop: A low noise Laser system for high fidelity Rydberg atom manipulation, TU Munich. (2019)
- [Did16] DIDACTIC, LD: *Fabry Perot Resonator*. 4747103. Leybold, 2016
- [HMIK15] HOSOYA, Toshiyuki ; MIRANDA, Martin ; INOUE, Ryotaro ; KOZUMA, Mikio: Injection locking of a high power ultraviolet laser diode for laser cooling of ytterbium atoms. In: *Review of Scientific Instruments* 86 (2015)
- [Iiz02] IIZUKA, Keigo: *Elements of Photonics, Volume I: In Free Space and Special Media*. John Wiley and Sons, 2002
- [Mes08] MESCHEDE, Dieter: *Optik, Licht und Laser*. 3. Vieweg Teubner, 2008
- [MOJ85] MOGENSEN, F. ; OLESEN, H. ; JACOBSEN, G.: Locking conditions and stability properties for a semiconductor laser with external light injection. In: *IEEE Journal of Quantum Electronics* 21 (1985), Nr. 7, S. 784–793. <http://dx.doi.org/10.1109/JQE.1985.1072760>. – DOI 10.1109/JQE.1985.1072760
- [MS07] METCALF, H.J. ; STRATEN, P. van d.: *Laser cooling and trapping of neutral atoms*. Wiley Online Library, 2007
- [Raz03] RAZAVI, Behzad: A Study of Injection Pulling and Locking in Oscillators. In: *IEEE CUSTOM INTEGRATED CIRCUITS CONFERENCE* (2003)
- [SED19] SHIMASAKIA, Toshihiko ; EDWARDS, Eustace R. ; DEMILLE, David: Injection-locking of a fiber-pigtailed high-power laser to an external cavity diode laser via a fiber optic circulator. In: *Review of Scientific Instruments* (2019)
- [Sie86] SIEGMAN, A.: *Lasers*. University Science Books, 1986
- [Sil96] SILFVAST, William T.: *Laser Fundamentals*. Cambridge University press, 1996
- [SPSG16] SAXBERG, Brendan ; PLOTKIN-SWING, Benjamin ; GUPTA, Subhadeep: Active stabilization of a diode laser injection lock. In: *Review of Scientific Instruments* 86, 063109 (2016)
- [Sze81] SZE, S.M.: *Physics of Semiconductor Devices*. John Wiley and Sons, 1981
- [WH91] WIEMAN, Carl E. ; HOLLBERG, Leo: Using diode lasers for atomic physics. In: *Review of Scientific Instruments* 62, 1 (1991)
- [WYH⁺03] WANG, Q. ; YAN, L. ; HO, P.-T. ; WOOD, G. ; DUBINSKIY, M. ; ZANDI, B.: Mutual Injection Locking of Two Individual Nd:YVO₄ Lasers in a Compound Cavity. In: *IEEE Annual Conference of the Lasers and Electro-Optics Society* 2 (2003)
- [Zim19] ZIMMERMANN, Claus: *Vorlesungsskript zur Laserphysik*. 2019

8 ACKNOWLEDGEMENTS

8 Acknowledgements

After a few years of study, it was great to gain the freedom to work on a project in a way, which was not completely defined. With the help of all people in the ErLi lab, being stuck on part of the project was not frustrating at all, because there always was a straight forward solution from one of the members to be counted on.

For the time I had in the ErLi lab, I want to thank the following people:

- Christian Gross not only for the formal supervision but for all very helpful suggestions and interesting insights into ultracold atomic physics.
- Alexandre de Martino and Florian Kiesel for the extensive proof-reading of the report, the possibility to ask questions at any time and for teaching me an accurate daily time schedule of lunch and coffee breaks in the lab.
- Ludwig Müller and Gregor Winkler for their help, especially during the first weeks in the lab.
- All members of the ErLi team and the Potassium team for the fun times during lunch breaks and bringing even more accuracy to the daily lunch schedule.
- My brother Florian for another extended proofread and my mom Nadyeh for her genuine interest in the project and being strong during difficult times.
- After all, I want to thank all my friends and flatmates for always bringing back the summer after many hours spent in the dark!